SYNTHESIS OF A PHENYLETHYLTHIOUREA DERIVATIVE AS A POTENTIAL NON-NUCLEOSIDE INHIBITOR OF HIV-1 REVERSE TRANSCRIPTASE

ALFRED WANGUSI ODONGO

B.Sc., PGDE

(SC/PGC/21/08)

A THESIS SUBMITTED IN PARTIAL FULFILMENT OF THE REQUIREMENTS FOR THE DEGREE OF MASTER OF SCIENCE, UNIVERSITY OF ELDORET

2013

DECLARATION

Declaration by the candidate

This thesis is my original work and has not been presented for the award of a degree in any other university. No part of this thesis may be reproduced without prior permission of the author and/or University of Eldoret.

Signature……. Date……..….

ALFRED WANGUSI ODONGO

SC/PGC/021/08

Declaration by the supervisors

This thesis has been submitted for examination with our approval as University Supervisors.

Signature…… Date……

Dr. CLARE MUHANJI

University of Eldoret, Kenya

Signature…….. Date…….…….

Dr. MAURICE OKOTH

University of Eldoret, Kenya

DEDICATION

I dedicate this work to my wife Zipora and sons Ian, Enrico and Albin who endured loneliness during my long absence from home, but showed patience and love. Special dedication to my late parents, Musa and Florence who challenged me to aim at high academic levels. More so, to my late brother John who motivated me into this research. Above all, to the Almighty Father who has enabled me to reach this far.

ABSTRACT

The emergence of resistant strains of HIV-1 towards existing drugs has prompted a search for new compounds with good antiviral activity and favourable toxicological profile. This work reports the synthesis of a PETT derivative, *N*-[2-(4-Hydroxyphenyl)ethyl]-*N*'-[2-(5-bromopyridyl)]-thiourea (**15**), using 4-hydroxybenzaldehyde (**14**) as the starting reagent. This involved hydroxyl group protection of **14**, followed by a Henry-Aldol condensation in to nitrostyrene **18**, in 94% good yields. Subsequent reduction of the nitrostyrene and eventual Boc protection gave carbamate **20**. This intermediate reagent **20** was then debenzylated via hydrogenolysis to form **21**, which was then Boc deprotected to form a new aminophenol **22**. The novel target compound **15** was furnished in 57% yield via a coupling reaction between the new phenol carbamate **21** and a thiocarbonyl derivative **6.** X-ray diffraction structural determination of one of the intermediates, *N*-[(2(4-benzyloxyphenyl)ethyl]-tert-butylcarbamate, **20**, displayed unit cell parameters a = 11.040(3) Å, b = 5.0931(12) Å, c = 64.070(16) Å, α= 90°, β= 94.493(14)°, γ = 90°, Z=8 and cell volume 3591.4(16) $Å^3$. This compound was found to exist in discrete monomeric molecules held together by hydrogen bonds and other intermolecular interactions. Its two rings are not coplanar and each molecule showed a twisted conformation with angles between the least squares planes of the aromatic rings of (C16, C20, C2 and C6 = -15.8 (3) °. A docking model of the inhibitor into the NNIBP using AutoDock, revealed the formation of hydrogen-bonds between a thiocarbonyl group (C=S) of **15** and amino hydrogen of the Lys 101 side chain. Additionally, its stability was attributed to the π-π stacking interactions of its phenyl ring and the two aromatic rings of Tyr 181 and Tyr 188. This was evident in the estimated Free binding energy of -7.50 kcal/mol. The estimated Inhibition Constant, K_i of **15,** was found to be 3.18 μM (Temperature = 298.15 K).

TABLE OF CONTENTS

LIST OF FIGURES

LIST OF TABLES

LIST OF ABBREVIATIONS

AIDS	Acquired Immunodeficiency Syndrome
ABC	(1S, 4R)-4-[2-Amino–6-(cyclopropyl–amino) 9*H*- purin–9-yl]-2-cyclopentene-1-methanol succinate
α-APA	α-(2,6-Dichlorophenyl)-α-(2-acetyl-5-methylanilino)acetamide
AZT	3'-Azido-2', 3'-dideoxythymidine
Bn	Benzyl
DAPY	Diarylpyrimidine
DATA	Diaryltriazine
d_4T	2',3'–Didehydro–2',3–dideoxyuridine
ddC	2',3'- Dideoxycytidine
DDDP	DNA-dependent DNA polymerization
Ddl	2', 3' – Dideoxyinosine
DIEA	Diisopropylethylamine
DMF	Dimethylformamide
DNA	Deoxyribonucleric acid
FDA	Food and Drug Administration
(-) FTC	(-)-β-L-3'–dideoxy-5–fluorocytidine
Gp	Glycoprotein
HAART	Highly active anti-retroviral therapy
HEPT	1-[(2-Hydroxyethoxy)methyl]-6-(phenylthio)thymine
HI-236	*N*'–(5-Bromo-2-pyridyl)–*N*-[2-(2,5-dimethoxyphenyl)ethyl]thiourea
HIV-1	Human Immunodeficiency Virus type 1

HIV-2	Human Immunodeficiency Virus type 2
IR	Infrared spectroscopy
ITU	Imidoylthiourea
NMR	Nuclear magnetic resonance
NNI	Non-nucleoside inhibitor
NNIBP	Non-nucleoside inhibitor binding pocket
NNRTIs	Non-nucleoside reverse transcriptase inhibitors
PETT	Phenylethylthiazolylthiourea
RDDP	RNA-dependent DNA polymerization
RNA	Ribonucleic acid
RNase-H	Ribonuclease H
RT	Reverse transcriptase
THF	Tetrahydrofuran
TIBO	(+)–(S)-4,5,6,7-Tetrahydro–8-chloro-5–methyl–6-(3-methyl-2-butenyl)imidazo[4,5,ijk][1,4]benzodiazepine–2-(1*H*)–thione
TLC	Thin layer chomatography
TMS	Trimethylsilane
UV	Ultraviolet

ACKNOWLEDGEMENTS

I would like to express my sincere gratitude to my academic supervisors Dr. Clare Muhanji and Dr Maurice Okoth for all their assistance, advice and support during laboratory work and thesis preparation. It has been an immense source of learning.

I am grateful to Prof. Abiy of Department of Chemistry, Nairobi University, for NMR analysis of my samples. In equal measure, I appreciate the support I had from the department of Pure and Applied Chemistry, University of Strathclyde (UK) for facilitating X-ray and NMR analyses through Dr. Okoth and Dr. Lutta.

I am also grateful to the entire technical staff of the Department of Chemistry and Biochemistry, University of Eldoret, for advice, administrative and technical assistance throughout the laboratory sessions of this research.

Special gratitude goes to Moi University, for funding this research project through the Annual University research grants.

I cannot forget colleagues Rotich, Barasa, Nobert, Sarah, Kimutai, Bett, Nyinge, Makumba and many others who were a source of encouragement during some of the challenging moments of my research.

CHAPTER ONE

INTRODUCTION

1.1 Background information

The Human immunodeficiency virus (HIV) is the causative agent for acquired immunodeficiency syndrome (AIDS) (Prajapati *et al*., 2009). It is an RNA virus and a member of the *Retroviridae* by virtue of its genome, morphology and possession of reverse transcriptase (RT) enzyme (Douek *et al.,* 2009). It has an icosahedral shape and is made up of an outer and inner core. The outer core (viral envelope or membrane) consists of a lipid bilayer. Projecting from this surface are knob like protrusions (Fig 1.1**)** that are made up of glycoproteins gp120 and gp41 (Cooley and Lewin, 2003).

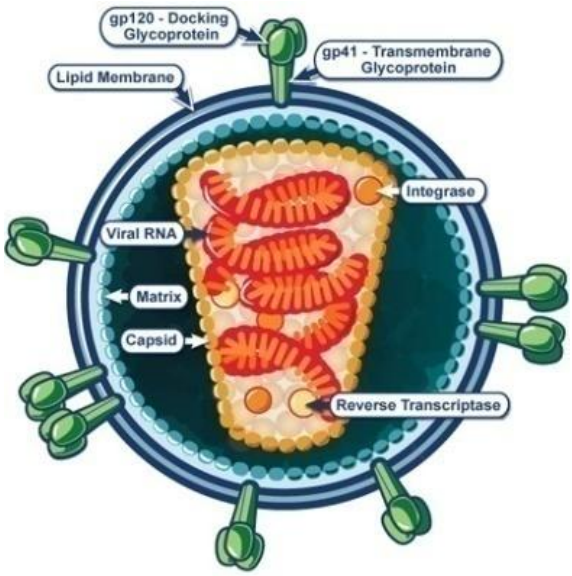

Fig 1.1: The structure of HIV (Niaid, 2011)

The HIV life cycle begins when the virus gets attached to the host cell membrane and ends with the release of new virions from the host cell (Mehellou and De Clercq, 2010). This process is catalysed by reverse transcriptase (RT) (Lodish *et al.*, 1995) (Fig 1.2**)**. It is an essential enzyme in the life cycle of HIV-1 and it is therefore the main target for the current anti HIV-1 drug research (Marsden and Zack, 2009).

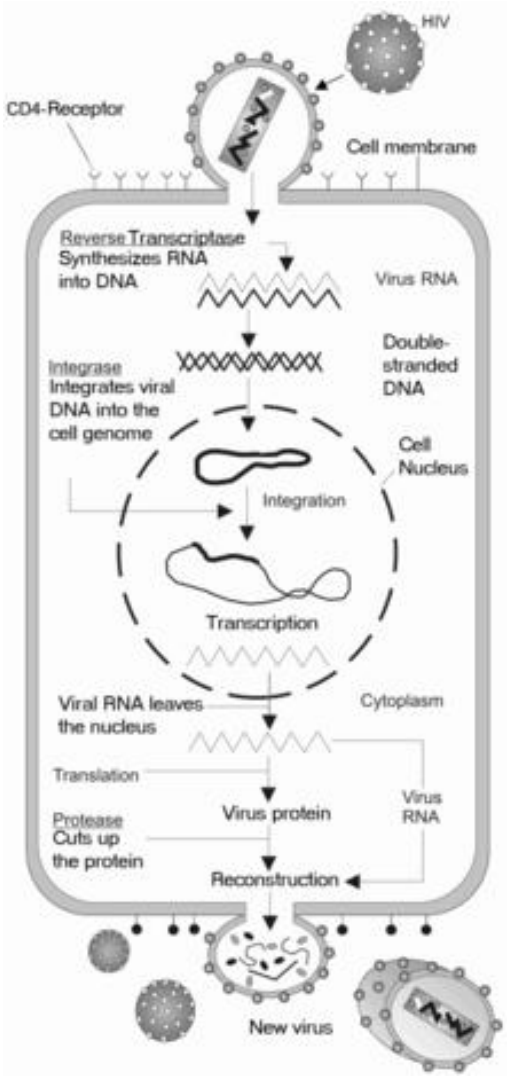

Fig 1.2: HIV-1 replication cycle (Lodish *et al.*, 1995)

1. 2 Crystallography

A crystalline solid is a material whose constituent particles (atoms, molecules or ions) display long-range order, built up from a regularly repeating pattern extending in all three dimensions. This pattern is located upon an array of points repeating periodically in the crystal motif. The array of points is referred to as a lattice and the points as lattice points. These lattice points form imaginary identical 'tiny boxes' called unit cells. The lengths of the edges of a unit cell (**a, b** and **c**) and the angles between them (α, β and γ) are called lattice parameters (Bryce *et al.,* 2000).

A crystal lattice can be thought to consist of these 'tiny boxes' stacked together in a three dimensional arrangement. The allowed translations of the unit cell contents create fourteen Bravais lattices, which belong to seven crystal systems. These are triclinic, monoclinic, tetragonal, orthorhombic, cubic, hexagonal and trigonal. These crystal classes differ from each other by having different relations between unit cell axes and angles (Table 1.1) (Bryce *et al.,* 2000).

Table 1.1: The seven crystal systems

Crystal system	Relations
Cubic	$a = b = c$, $\alpha = \beta = \gamma = 90^o$
Tetragonal	$a = b \neq c$, $\alpha = \beta = \gamma = 90^o$
Orthorhombic	$a \neq b \neq c$, $\alpha = \beta = \gamma = 90^o$
Monoclinic	$a \neq b \neq c$, $\alpha = \gamma$; $\beta \neq 90^o$
Triclinic	$a \neq b \neq c$, $\alpha \neq \beta \neq \gamma \neq 90^o$
Trigonal (Rhombohedral)	$a = b = c$, $\alpha = \beta = \gamma \neq 90^o$
Hexagonal	$a = b \neq c$, $\alpha = \beta$; $\gamma = 120^o$

1.2.1 Point groups and Space groups

In crystallography, a point group is a set of symmetry operations that leaves a central point fixed while moving other directions and faces of the crystal to the positions of features of the same kind. Such operations include rotation, reflection and inversion. These operations are characterised by leaving the macroscopic properties of a crystal virtually unchanged. The point group of a crystal, among other things, determines directional variation of the physical properties that arise from its structure, such as optical properties. A combination of all possible symmetry operations (point groups plus glides and screws) with the Bravais translations leads to the 230 Space Groups (Hahn, 2002).

1.2.2 Single crystal X-ray crystallography

X-ray crystallography is a powerful technique in determining the arrangement of atoms within a crystal. In this technique, a beam of X-rays strikes a crystal thus causing it to spread into many specific directions (Yang *et al.*, 2007). From the angles and intensities of these diffracted beams, one can produce a three dimensional structure of the density of electrons within the crystal. Vital information such as mean positions of the atoms in the crystal, chemical bonds and their disorder can be deduced from the electron density. X-ray crystallography has also been used to obtain geometrical data such as bond angles, bond lengths, and torsion angles of spirobinaphthopyrans (Linda *et al.*, 1999), as well as the conformation and shapes of molecules in a crystalline structure (Bryce *et al.*, 2000).

1.3 Statement of the problem

An estimated 1.8 million AIDS related deaths have been reported, in addition to the 34 million people currently living with HIV worldwide. A vast majority of these cases, 22.9 million people who live with the virus are residents of Sub-Saharan Africa. They represent 68% of the world's HIV infected population. The region also accounts for 70% of new HIV infections (UNAIDS, 2011). Whereas Sub-Saharan Africa remains the region most heavily affected, Asian countries have the lowest HIV prevalence rates of less than 1%. Interestingly, in countries like Australia, with an HIV prevalence of 0.2%, the per capita rate of HIV diagnosis in 2006–2008 was more than eight times higher among immigrants from sub-Saharan Africa than among

Australian-born persons (National Centre in HIV Epidemiology and Clinical Research, 2009). The pandemic has not spared any gender, with women having a higher HIV prevalence rate as compared to men. A good example is the case of sub-Saharan Africa, where women account for about 60% of the estimated HIV infections (UNAIDS, 2011). It is therefore clear that HIV/AIDS pandemic continues to pose a medical predicament (UNAIDS, 2011) with no known cure (Prajapati *et al.*, 2009).

1. 4 Justification of the study

The efficacy of current anti-retroviral drugs used has suffered drawbacks due to the emergence of resistant strains of HIV-1. Moreover, some drugs have been associated with severe side effects (Prajapati *et al.*, 2009) prompting the need for further refinement of the existing antivirals into compounds with high activity against both wild type and mutated forms of the virus, low toxicity and good pharmacokinetic properties (Daelemans, 2010). Such compounds include a class of NNRTIs called phenylethylthiazolylthiourea (PETT) derivatives, which are known for their good antiviral activity and favourable toxicological profile (Christer *et al*., 1998).

Additionally, understanding the internal structure of the crystals of some of the compounds synthesized is important for theoretical purposes and also contributes towards increasing the number of structures whose crystallographic information is known. Although the crystallographic data of two of the intermediate compounds has been availed (Kennedy *et al.*, 2010[a] and Kennedy *et al.*, 2010[b]), single crystal X-ray

diffraction for the synthetic intermediate; *N*-[(2(4-benzyloxyphenyl)ethyl]-*tert*-butylcarbamate has not been explored. This was done so as to determine the success of its synthesis as well as to make known its crystallographic data.

1.5 Objectives

The objectives of this study were;

1. To synthesize *N*-[2-(4-hydroxyphenyl)ethyl]-*N*'-[2-(5-bromopyridyl)]-thiourea from 4-hydroxybenzaldehyde using a series of steps.

2. To explore structural details of *N*-[(2(4-benzyloxyphenyl)ethyl]-*tert*-butylcarbamate; an intermediate obtained during the synthesis of the target compound.

CHAPTER TWO

LITERATURE REVIEW

2.1 The reverse transcriptase enzyme (RT)

Reverse transcriptase (RT) is the replicative enzyme of HIV and other retroviruses. It converts single stranded RNA of HIV into double-stranded DNA which is subsequently integrated into the host cell DNA (De Clercq, 2009). HIV-1 RT is composed of two subunits, p66 and p51. A p66 subunit has 560 amino acid residues while p51 has 440 amino acid residues (Kitchen *et al.,* 2001). The p66 subunit contains two domains; polymerase and RNaseH, while p51 lacks the RNaseH domain. The polymerase domain in both p66 and p51 contains four common sub-domains named as fingers, palm, thumb and connection (Fig 2.1). The nucleic acid cleft extends from the polymerase active site to the RNaseH active site in the p66 subunits. The p51 subunit is not directly involved in the catalytic activity of RT enzyme but instead provides structural support that allows the p66 subunit to carry out polymerase and RNaseH activities (Carr, 2003).

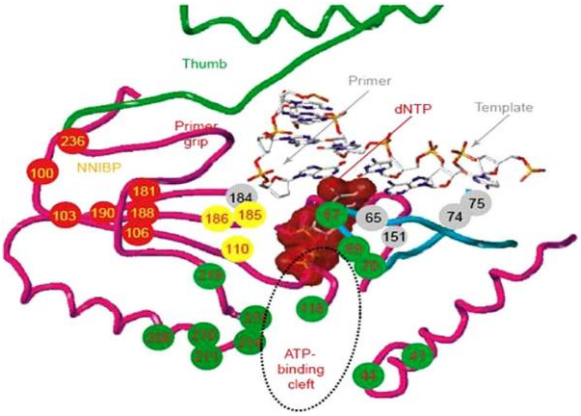

Fig 2.1: HIV-1 RT structure in the region near the polymerase active site (Sarafianos *et al.*, 2004)

2.2 HIV-1 reverse transcriptase inhibitors

Drugs that inhibit the functions of reverse transcriptase enzyme are known as reverse transcriptase inhibitors. They constitute two types: nucleoside reverse transcriptase inhibitors (NRTIs) and non-nucleoside reverse transcriptase inhibitors (NNRTIs) (Mehellou and De Clercq, 2010)

Nucleoside reverse transcriptase inhibitors (NRTIs) are drugs that in their triphosphate form, bind at the polymerase active site and bring about termination of growth of the DNA chain upon incorporation into the primer strand (Huang *et al.*, 1998). This is mainly due to the fact that NRTIs lack the 3'-hydroxyl group, hence preventing the incorporation of the incoming nucleotide (Hershhorn, 2008). The resultant effect is termination of synthesis of the DNA primer strand (Venkatachalam *et al.*, 2004). NRTIs are therefore competitive inhibitors of the HIV RT enzyme (Das

et al., 2005). Currently, six NRTIs; namely, Azidovudine (AZT), dideoxycytidine (ddC), Abacavir (ABC), didanosine (ddI), Emtricitabine (FTC) and Lamivudine (3TC) (Fig 2.2) have been approved by the US Food and Drug Administration for the treatment of HIV (Mehellou and De Clercq, 2010 and De Clercq, 2010[b]).

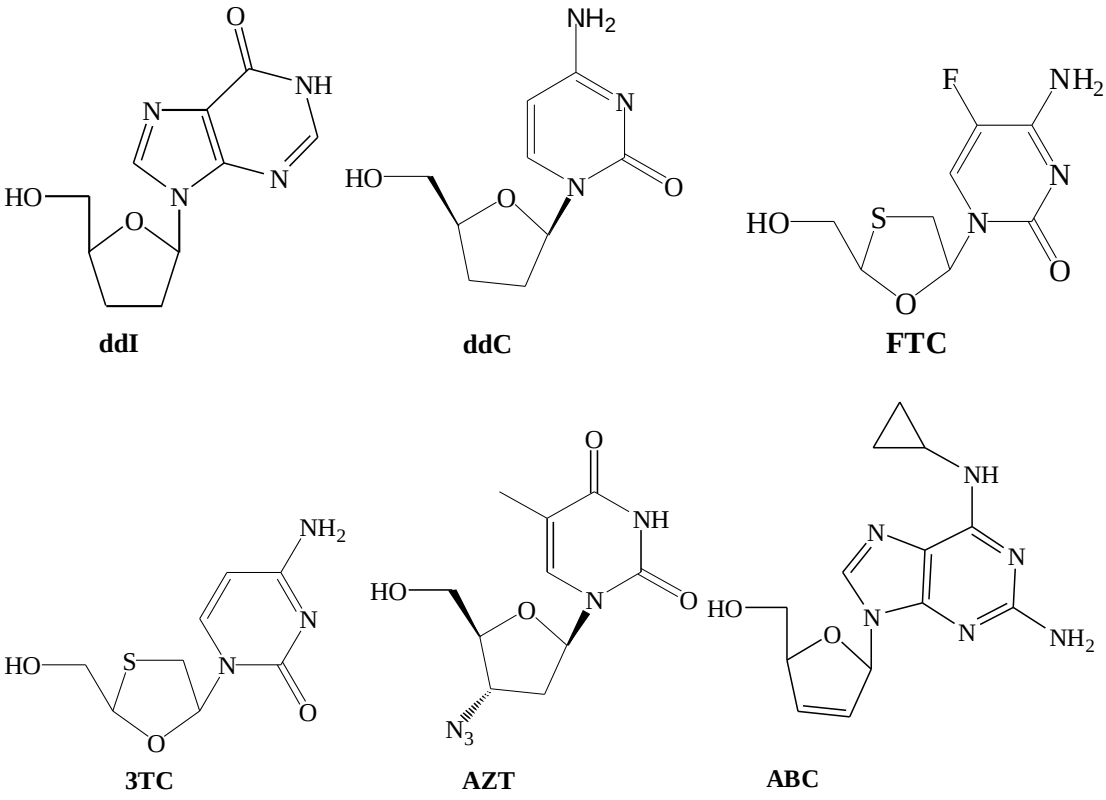

Fig 2.2: Current FDA approved NRTIs (Mehellou and De Clercq, 2010).

On the other hand, non nucleoside reverse transcriptase inhibitors are a variety of compounds that inhibit HIV reverse transcriptase by binding to an allosteric site and this in turn leads to either conformational or mobility changes (or both) (Ren *et al*.,

2007). The allosteric site is located near but separate from the polymerase active site (Pauwels, 2004). Since the discovery of HEPT and TIBO as specific inhibitors of HIV-1 RT, a large number of NNRTI compounds have been reported including but not limited to TIBO [8-chloro-TIBO (Tivirapine)], HEPT derivatives (MKC-442), dipyridodiazepinone (Nevirapine), pyridinones (Fig 2.3), BHAP derivatives (Delavirdine), TSAO derivatives, PETT derivatives (Trovirdine), thiazolobenzilimidazole, thiocarboxanilide derivatives, and quinoxaline derivatives among others (De Clercq, 2009).

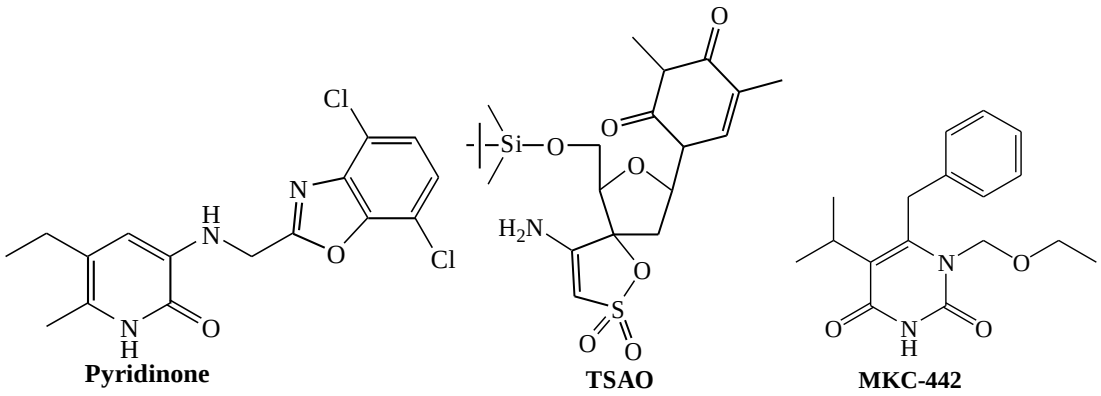

Fig 2.3: Chemical structures of NNRTIs (De Clercq, 2009).

Though NNRTIs are characterized by high chemical diversity, they all bind at the same site in the RT and the overall shape of the non-nucleoside inhibitor binding pocket (NNIBP) (Fig 2.4) does not vary to a significant extent, despite their ligands being chemically different (Balzarini, 2004).

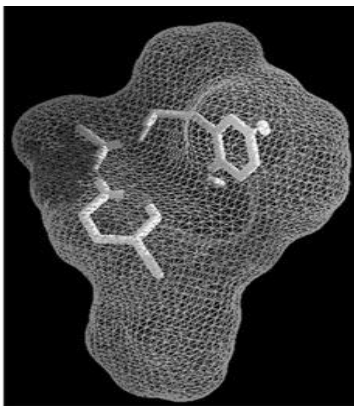

Fig 2.4: The HI-236 molecule in the NNIBP. (de Béthune 2010)

2.3 NNRTI Resistance

NNRTIs are highly specific and commonly trigger the emergence of viral mutants that are drug resistant especially due to a monotherapy treatment regimen. Mutations arise from numerous errors which are made by the HIV-1 RT and these mistakes remain uncorrected due to the absence of 3'-exonuclease proof reading activity during DNA synthesis. This results in an average error rate per detectable nucleotide incorporated of 1/1700 (Roberts *et al.*, 1998). This is worsened by the high replication rate of the virus with the production of 1 to 10 billion new virus particles per day in an infected individual not on treatment (Perelson and Ribeiro, 2008), it can be deduced that mutant type of HIV is always present. It is these mutations that cause resistance to NNRTIs. The most common mutations occur at Y181 and/or Y188 within HIV-1 RT resulting to very high level resistance against many first generation NNRTIs like

Nevirapine. An example to illustrate this is where tyrosine is mutated to cysteine at positions 181 and 188 (which correspond to Y181C and Y188C mutations respectively). The resultant effect of these changes is the loss of aromaticity and hence a decreased or loss of interactions with the inhibitors (Ren *et al*., 2001). On the other hand, the L100I and G190A mutations bring about resistance due to steric variations. Such mutations will severely impair the potency of rigid NNRTIs like Nevirapine and α-APA (Lindberg *et al*., 2002).

2.4 The development of non-nucleoside reverse transcriptase inhibitors

The era of NNRTIs began in the late 1980s with the discovery of 1-(2-2-hydroxymethyl)-6-(-6-(phenylthio)thymine (HEPT) (Baba *et al*., 1989), and tetrahydroimidazo[4,5,1-jkj][1,4]benzodiazepin-2(1H)-one and -thione (TIBO) (Fig 2.5) compounds (Debyser *et al*., 1991) following an MT-4 cell-based anti-HIV random screening program by Janssen Pharmaceutica, in collaboration with the Rega Institute (Pauwels *et al.,*1990). These compounds were unexpectedly found to inhibit RT, with HEPT displaying a moderate activity against HIV-1 replication (IC_{50} = μM) (Miyasaka *et al.,* 1989). This prompted studies on the mechanism of their action. Although HEPT compounds had been described before TIBO compounds, they were initially thought to be NRTIs. However, it was later revealed that they shared a common mechanism of action (de Bethune, 2010 and De Clercq, 2010[a]).

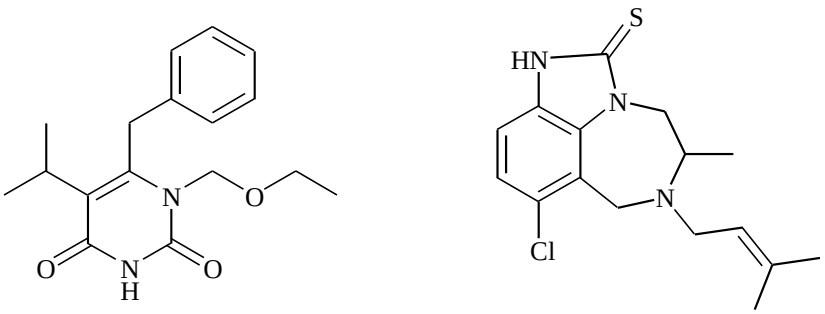

HEPT (MKC-442) **TIBO**

Fig 2.5: NNRTIs HEPT and TIBO.

Following these discoveries, screening methods were done, leading to the development of other NNRTIs.

2.4.1 First generation NNRTIs

Nevirapine (De Clercq, 2009) a dipyridodiazepinone, which inhibited viral RT activity by a non-competitive mechanism (with respect to dNTP binding) showed high efficacy, as indicated by the improved control of virus replication and immunologic profile among patients (Lange, 2003). It was thus approved in 1996 by FDA for clinical use. However, when administered to patients as a monotherapy, it led to the emergence of a resistance profile that would currently not be acceptable (Harris, 2003). It is therefore recommended for use in combination with two NRTIs as first line therapy in developing countries (Guay *et al.*, 1999). Since then, several families of NNRTIs have been developed following intensive research leading to approval of Delavirdine in 1997 and Efavirenz in 1998 (Fig 2.6) by the FDA (de

Béthune, 2010). To date, Nevirapine and Efavirenz are cornerstones of first line highly-active anti-retroviral therapy (HAART), whereas Delavirdine is rarely used due to its relatively poor resistance profile (de Bethune, 2010). Studies done on crystals of these first generation NNRTIs (like TIBO, Nevirapine and α-APA) complexed with RT revealed that they bind HIV-1 RT in a "butterfly-like" conformation. They were nevertheless, found to be prone to drug-resistant mutations. This triggered the need for discovering new compounds with higher efficacy (Monforte *et al*., 2009).

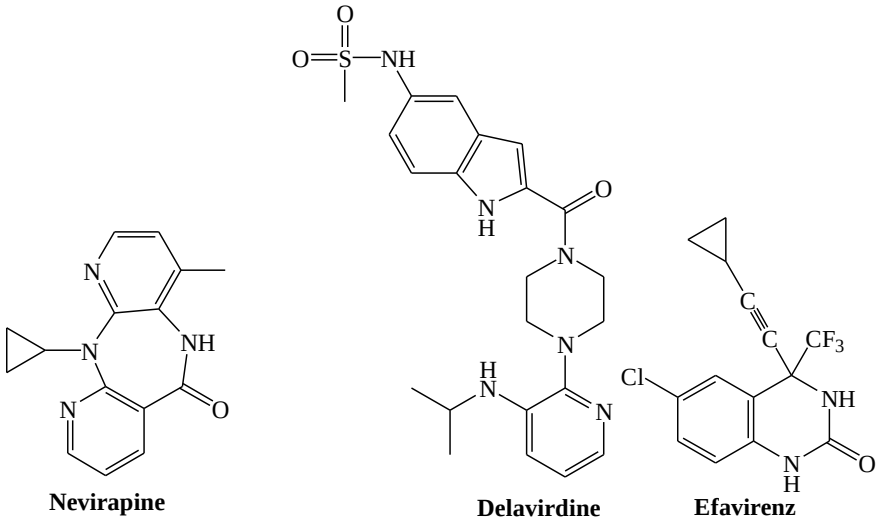

Fig 2.6: Chemical structures of first generation NNRTIs approved by FDA.

2.4.2 Next generation NNRTIs

The first generation NNRTIs are characterized by possession of rigid structures while exhibiting a “butterfly-like” conformation in the NNIBP. On the other hand, the second generation analogues are structurally flexible and adopt a “horseshoe” conformation in the inhibitor binding pocket. This flexibility is very crucial when it comes to adapting to the plasticity and changes of the NNIBP, which is in turn critical for potency against wild type and mutant strains of HIV-1 (Li *et al*., 2012). This very potential series of NNRTIs, emerged *via* modifications done on α-APA analogs to give rise to Imidoylthiourea (ITU) (Fig 2.7).

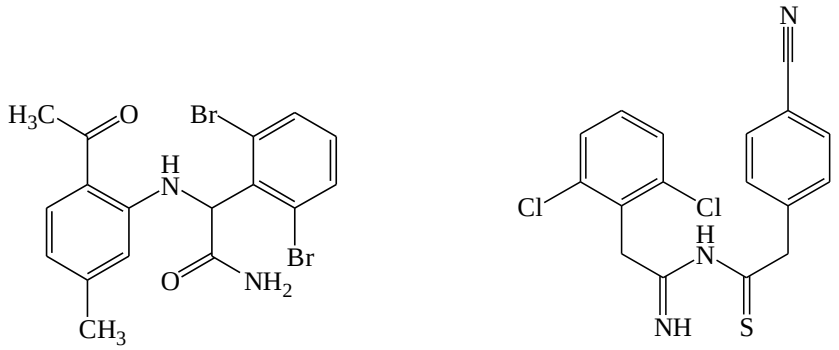

(a) Loviride **(b) R100943 (ITU)**

Fig 2.7: Some of the first generation NNRTIs (a) α-APA analogue (Loviride) and (b) ITU (R100943)

This was achieved by extending the linker that binds the aryl side groups of the α-APA. A potent ITU compound, R100943, obtained exhibited a "U" or “horseshoe” mode of binding and was found to be more flexible than α-APA. The compound

inhibited HIV-1 and was considerably effective against a number of key NNRTI-resistant mutants such as G190A, which had caused high-level resistance to Loviride (α-APA) and Nevirapine (Samuele *et al*., 2009). However, the potency of R100943 against HIV-1 resistant mutants (like Y181C and Y188L/H) was relatively inadequate, in addition to the chemical instability of the imidoylthiourea part of the ITU derivative. It was therefore found not to be favorable for an oral drug (Das *et al.*, 2005). Nonetheless, the ITU derivative had shown an improved resistance profile owing to its torsional freedom and thus compensated for the effects of resistance mutations (De Corte, 2005). In an effort to obviate its lability issue, the unstable imidoylthiourea moiety was replaced with a cyanoguanidine bioisostere, which resulted in an unanticipated ring closure (Scheme 2.1). This furnished a remarkably stable diaryltriazine (DATA) derivative R106108 with similar activity as ITU. Crystal structure analysis revealed that DATA compounds could bind the NNIBP in various modes, which made them stronger against drug-resistant mutations (Ludovici *et al.*, 2001).

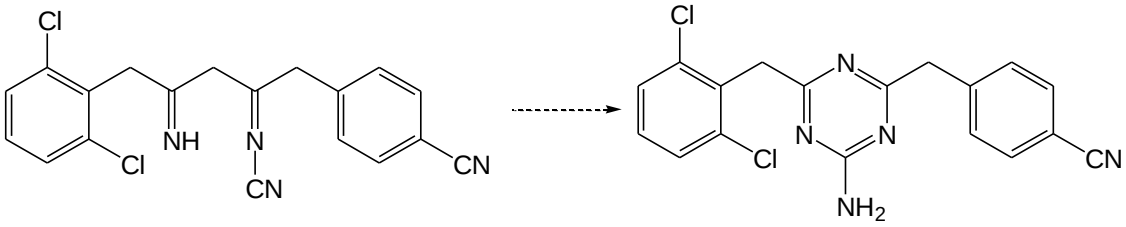

ITU bioisostere

R106108

Scheme 2.1: Unexpected ring closure: ITU to DATA derivative R106108

The search for more potent drugs saw the modification of DATA compounds into a new class of compounds called diarylpyrimide (DAPY). They were made by the replacement of the central triazine ring from the DATA compounds, with a pyrimidine (Fig 2.8).

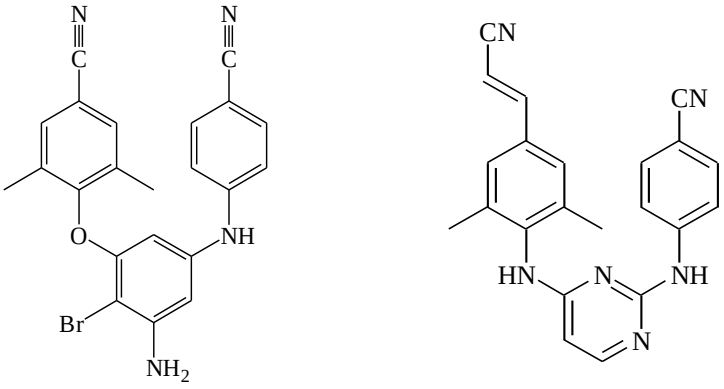

Etravirine **Rilpivirine**

Fig 2.8: The chemical structures of the highly active next generation NNRTIs approved by FDA

This new class exhibited a higher anti-HIV activity against drug resistant HIV-1 strains compared to the corresponding DATA analogs. An example of the DATA analogues is etravirine, which proved to be highly active against HIV-1 and many of its clinically prevalent mutants with an IC_{50} below 10 nM (Seminari *et al.*,2008) and was eventually approved in 2008 by the FDA (Schiller and Youssef-Bessler, 2009; Maga *et al*., 2010).

Further optimization of DAPY compounds led to the discovery of rilpivirine, which had a superior antiviral profile (IC_{50} less than 5 nM) as well as a better bioavailability profile compared to other NNRTIs. This was partly attributed to the extended cyanovinyl group which makes strong contacts with the highly conserved W229

(Janssen *et al.,* 2005). Phase III studies revealed that rilpivirine had similar efficacy as efavirenz but with less side effects. Following this excellent display of antiretroviral activity, rilpivirine was thus approved for clinical use by the FDA in 2011 (Li *et al*., 2012).

2.5 PETT derivatives as anti-HIV compounds

The continued search for anti-HIV-1 compounds saw the emergence of another class of NNRTI compounds known as phenethylthiazolylthiourea (PETT) derivatives. A PETT molecule can be viewed as one consisting of two groups attached to a thiourea group. One side of the molecules is either a 2-aminothiazole group (PETT) or a 5-bromopyridyl group as in the case of trovirdine (Fig 2.9). Both these groups are capable of forming an intramolecular hydrogen bonded heterocyclic ring. The other side of the molecule is either a pyridyl or phenyl ring joined to the thiocarbonyl group by an ethyl linker (D'Cruz and Uckun, 2005).

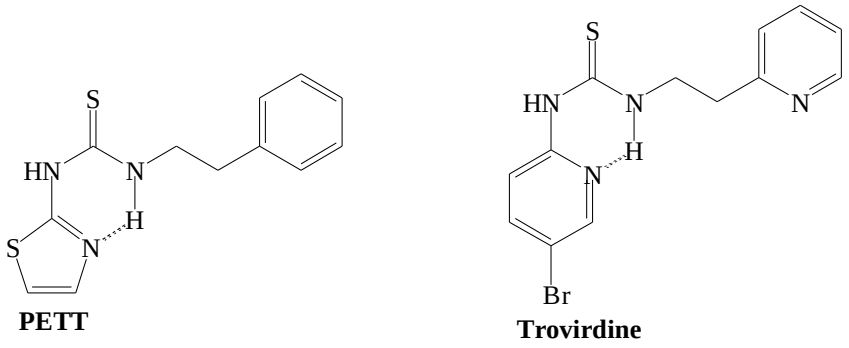

PETT **Trovirdine**

Fig 2.9: PETT derivative and trovirdine

These compounds were first synthesized by Bell *et al*., (1995) and Cantrell *et al.*, (1996) as potent inhibitors of HIV-1 RT. One of the methods involved the condensation of the amine **4** with thiourea derivative **3** to furnish PETT derivative **5**. Reagent **3** was derived from the condensation of 2-aminothiazole **2** with thiocarbonyldiimidazole **1** (Scheme 2.2).

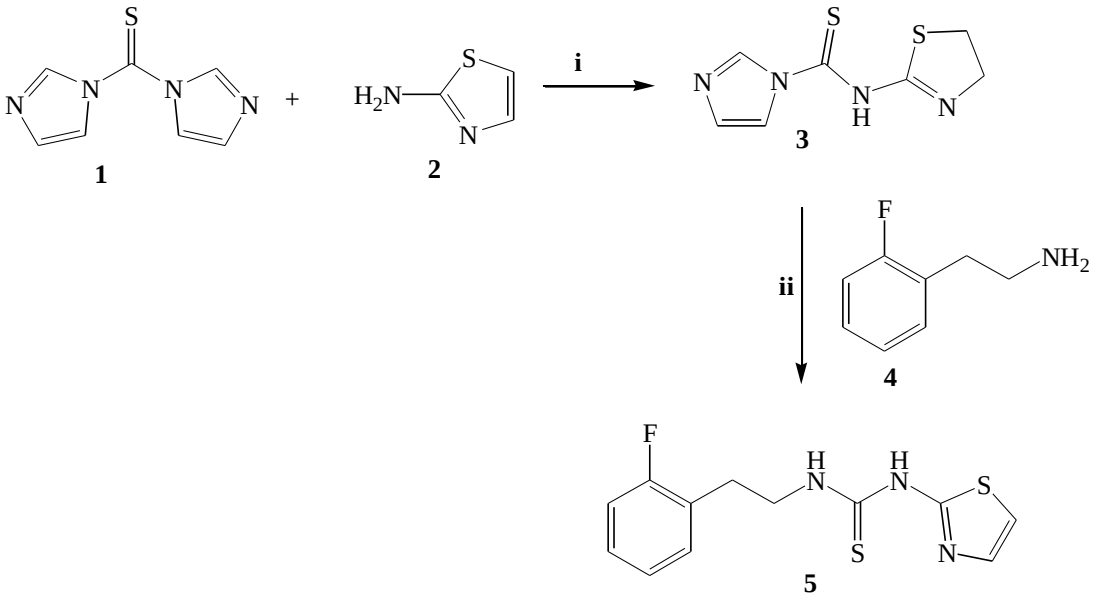

Scheme 2.2: *Reagents and conditions:* (**i**) CH_3CN, rt, 12 h. (**ii**) DMF, 100 ℃, 16 h.

Since then, a number of studies have been carried out on this class of compounds and their interactions with NNIBP. For example, through modelling studies, spatial gaps surrounding the pyridyl ring of the active PETT derivative, Trovirdine were discovered in the NNIBP (Mao *et al*., 1998). Following this, a planar ring of Trovirdine was replaced with a larger non planar piperadinyl or piperazinyl ring. This

was done so as to optimize occupancy of the spacious wing 2 region of the "butterfly" shaped non-nucleoside inhibitor binding pocket (NNIBP).

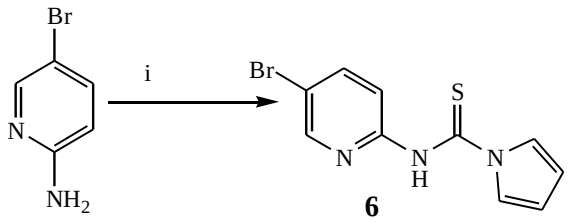

Scheme 2.3: *Reagents and Condition*: (**i)** 1,1'-thiocarbonydiimidazole, acetonitrile, rt, 12 h.

Two compounds were thus obtained following the method for synthesis of PETT derivatives developed by Bell *et al.,* (1995). The synthetic process involved condensing 2-amino-5-bromopyridine with 1,1'-thiocarbonyldiimidazole to form a thiourea reagent **6**, (Scheme 2.3). The target compounds **8** and **10** were achieved by condensation of amines **7** and **9** with the thiourea derivative **6,** respectively (scheme 2.4).

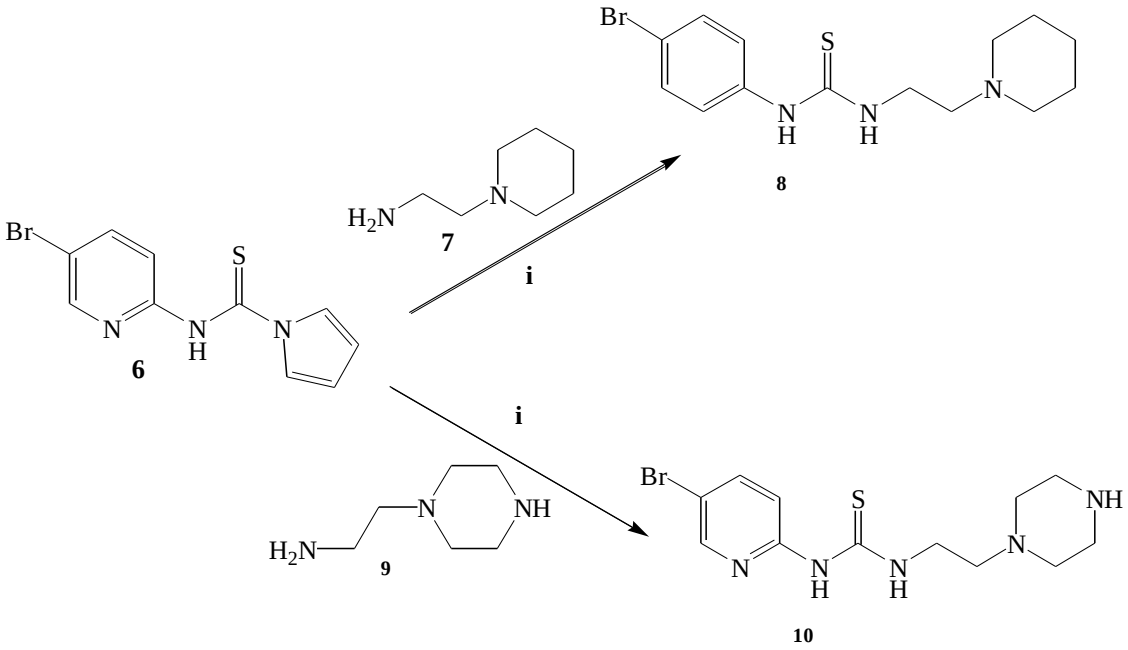

Scheme 2.4: *Reagents and Conditions:* (**i)** DMF, 100 ℃, 15 h.

The anti-HIV activities of the two heterocyclic compounds were determined and found to be more potent than Trovirdine and inhibited HIV replication at nanomolar concentrations, with no evidence of cytotoxicity (Mao *et al.*, 1998). However, the two PETT analogues were inactive against the resistant variants of HIV-1, thus inferior to Trovirdine (Mao *et al*., 1999).

In an effort to maximize occupancy of the extra space in the NNIBP, molecular modeling studies using computational approach were done on Trovirdine, leading to the discovery of HI-236. This new PETT analogue was associated with enhanced anti-HIV-1 activity even against drug resistant

mutants. Its synthesis involved condensation of thiourea reagent **6** with amine **11,** furnishing HI-236, **12** (Scheme 2.5) in good yields (Hogberg *et al.*, 2000).

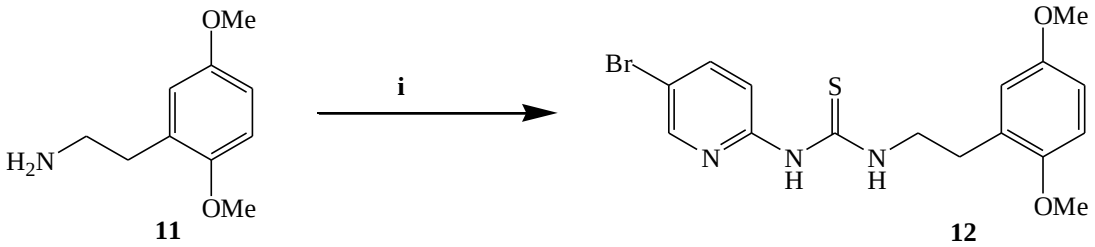

11 **12**

Scheme 2.5: *Reagents and Conditions*: (**i**) DMF, 100℃, 16h, (40%).

In another attempt to improve the anti-HIV activity of HI-236, a small library of fifteen compounds was obtained by attaching different tethers at the C-2 phenolic oxygen of HI-236 and their anti-HIV activities determined. Compounds **13** and **14** (Fig 2.10) with a butynyl and a hydroxyethyl tethers showed higher activities of 0.026 and 0.012 µM respectively, compared to 0.048 µM for HI-236 (Hunter *et al*., 2008).

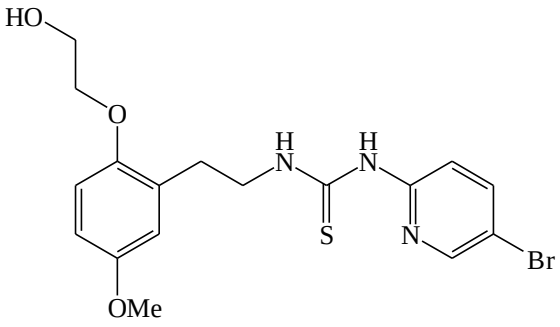

13

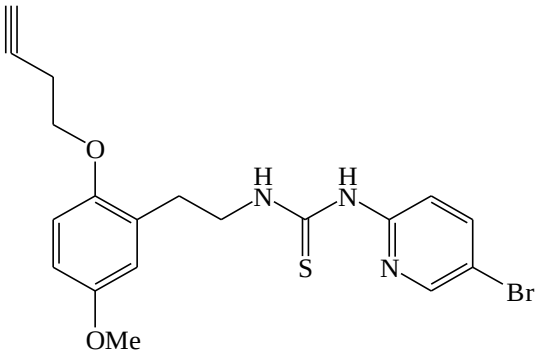

14

Fig 2.10: HI-236 derivatives

2.6 Crystallography of PETT compounds

X-ray crystallography is currently used consistently by researchers to determine how a drug or a candidate drug interacts with its protein target as well as what changes might improve it (Scapin, 2006). An instant to illustrate this is where co-crystals of HIV-1 RT complexes with NNRTIs (Fig: 2.11) have been used to study the nature of NNIBP and the various modes of inhibitor binding (Das *et al*., 2005). This has in turn contributed to the great strides made towards the discovery and development of NNRTIs, including PETT derivatives. In equal measure, crystallographic studies of

individual compounds have contributed to the understanding of their orientation in the NNIBP. An example is a research by Venkatachalam *et al.*, (2005) in which the structural anisotropy of thiourea derivatives in the solid state was found to depend on the substituents attached.

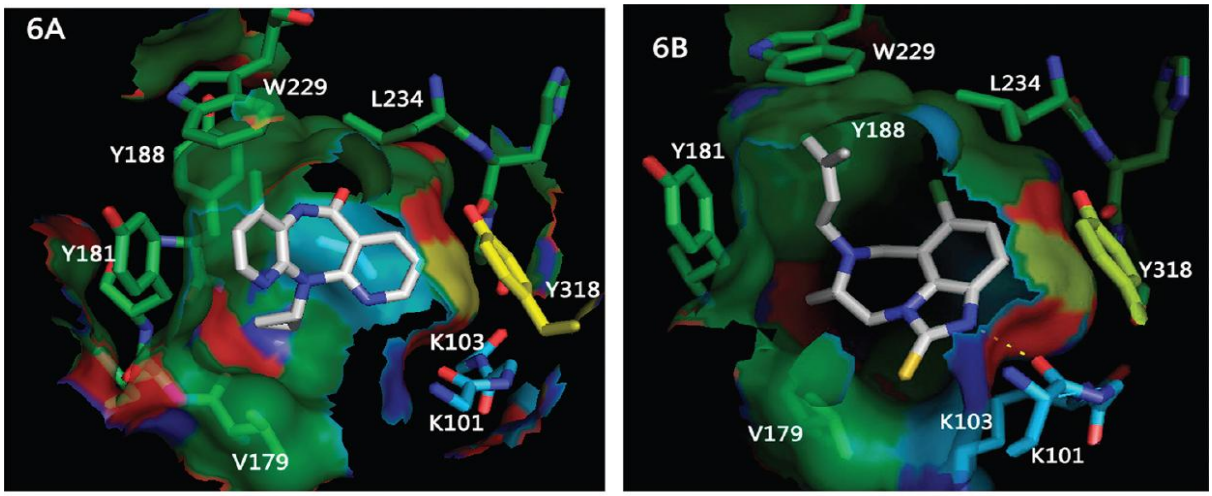

(A) (B)

Fig 2.11: (A) X-ray crystallographic structure of RT/nevirapine complex (B) X-ray crystallographic structure of RT/TIBO 12 complex (Ding *et al.*, 1995).

2.7 Crystallography of synthetic intermediates of PETT derivatives

In an attempt to synthesize a PETT analogue, Rotich (2010) had two of the intermediates, 4-(benzyloxy)benzaldehyde, **17** and 2-(4-benzyloxyphenyl)-1-nitroethene, **18** structures analysed by X-Ray crystallography (Fig. 2.12) (Kennedy et al., 2010[a] and Kennedy *et al.*, 2010[b]).

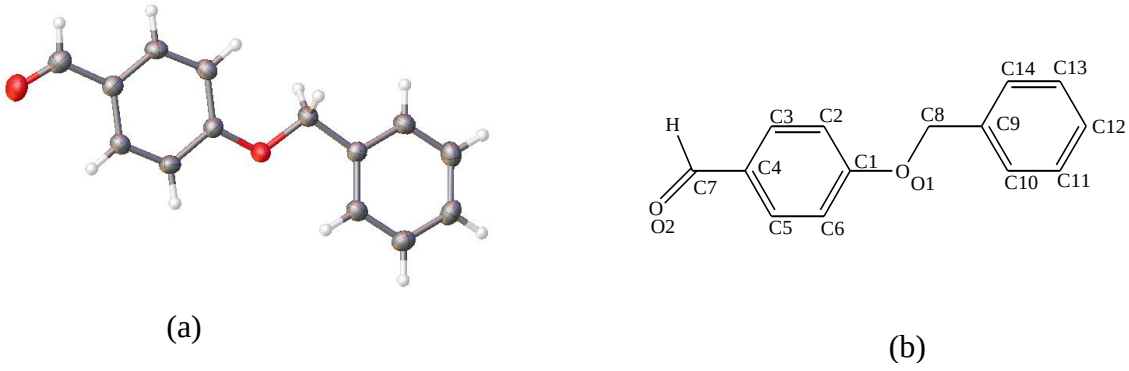

(a) (b)

Fig 2.12: (a) X-ray skeletal structure of compound 17 (b) Skeletal structure of compound 17 with labels (Rotich, 2010).

The compound **17**, was found to exist in discrete molecules, which are packed in such a way that four molecules are located in one unit cell of the crystals of this compound (Z=4) (Fig 2.13).

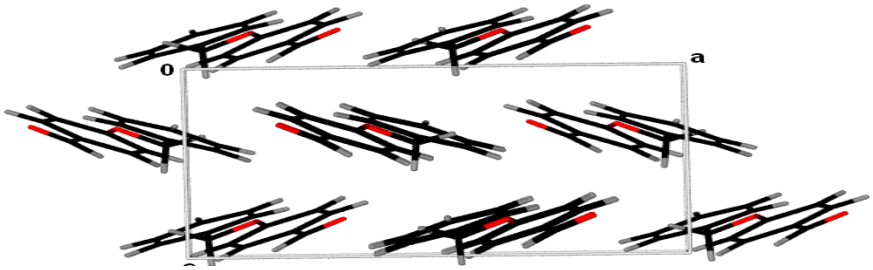

Fig 2.13: Molecular packing in the crystals of 4-(benzyloxy)benzaldehyde (Kennedy *et al.*, 2010[a])

In every unit cell, molecules were arranged in a particular direction within a given line and an opposite orientation observed in the neighbouring lines (Fig. 2.13). This

pattern pointed out to the existence of organized intermolecular hydrogen bonding (Kennedy *et al.*, 2010[a]).

The second synthon, **18,** was observed to exist as a trimer (Fig 2.14), in which three independent molecules per asymmetric unit are held together by weak Van der Waals forces. Each molecule exhibited a twisted conformation with torsion angles between the planes of the aromatic rings of 70.25˚, 72.33˚ and 84.21˚ respectively. Both the trans- olefin and the nitro- groups lie in the plane of their attached aryl ring (CCCC torsion angles -0.8, 1.1 and 6.6 degrees; CCNO torsion angles -5.9˚, -2.5˚ and 9.7˚) (Kennedy *et al.*, 2010[b]).

.

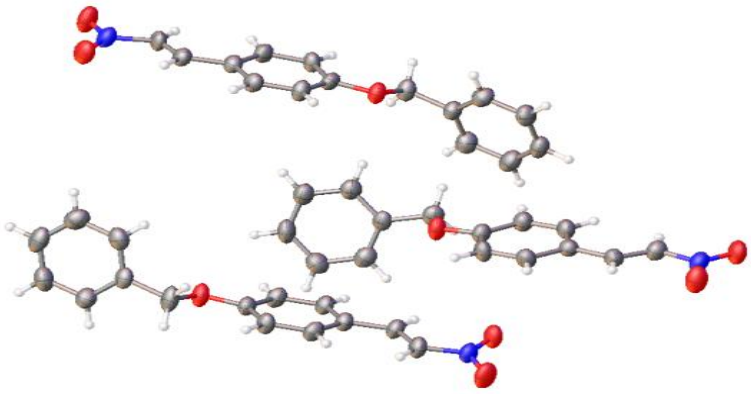

Fig 2.14: X-ray skeletal structure (Kennedy *et al.*, 2010[b])

CHAPTER THREE

EXPERIMENTAL

3.1 General Procedures

All reactions were performed in oven-dried glassware under an inert atmosphere of dry nitrogen. The following reagents and solvents were purchased from Sigma-Aldrich: di-*tert*-butyldicarbonate, trifluoroacetic acid, dimethylformamide (DMF), anhydrous potassium carbonate, nitromethane, diisopropylethylamine (DIEA), lithium aluminium hydride (LAH), tetrahydrofuran (THF), triethylamine, acetonitrile (HPLC), anhydrous magnesium sulfate, dichloromethane (AR), petroleum ether (AR), benzyl bromide (AR), 10% palladium on carbon, 2-amino-5-bromopyridine, ammonium acetate, 1,1'-thiocarbonyldiimidazole, ethanol (AR), ethyl acetate (AR), zinc granules, 4-hydroxybenzaldehyde, and hydrochloric acid.

^{1}H NMR and ^{13}C NMR spectra were recorded using a Varian 200 MHz NMR spectrometer at the Department of Chemistry, University of Nairobi, Kenya and Strathclyde University, UK. IR analyses were done on a Shimadzu IR 408 spectrometer. TLC plates (Merck) were used to monitor the progress of reactions during synthesis and visualized under UV light. Column chomatography was performed using Fluka silica-gel 60 (70-230 mesh) as the stationary phase. All reactions were carried out under nitrogen gas.

4-(Benzyloxy)benzaldehyde (17)

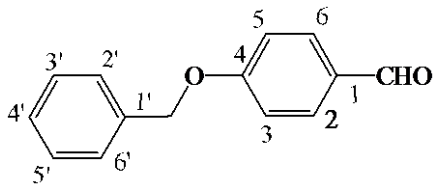

A solution of 4-hydroxybenzaldehyde **16** (5.00 g, 41.0 mmols), benzyl bromide (7.31 mL, 61.5 mmols) and anhydrous K_2CO_3 (20.00 g, 144.3 mmol) in ethanol (5 mL) were stirred at reflux for 3 h. The reaction mixture was cooled then filtered though a pad of Celite and washed with large volumes of EtOAc and the solvent removed under reduced pressure. The residual mass was washed twice with 10 mL portions of saturated NaCl, aqueous sodium hydroxide (5%) and water. The Et_2O solution was dried over anhydrous $MgSO_4$, evaporated under reduced pressure and the crude product recrystallized from EtOH to yield colourless crystals (8.24 g, 95%). mp 71 – 74 ˚C (Lit. 71 – 74 ˚C) (Rotich., 2010), IR: 1685 cm^{-1} (s) (C=O), 1260 cm^{-1} (w) (C-O-C). ^{1}H NMR ($CDCl_3$, 200 MHz): δ 7.42 (5H, m, H2', H3', H4', H5' and H6'), 7.26 (2H, d, J = 8.6 Hz, H2 and H6), 7.02 (2H, d, J = 8.6 Hz, H3 and H5), 5.13 (2H, s, $ArCH_2O$), 10.51 (1H, s, CHO). ^{13}C NMR ($CDCl_3$ 50 MHz): δ 190.0 (CHO), 137.0 (C-1), 135.4 (C-4), 135.3 (C-1'), 131.4 (C-2, C-6), 129.1 (C-2', C-6'), 128.6 (C-4'), 128.0 (C-3', C-5'), 116.0 (C-3, C-5), and 70.5 ($ArCH_2O$).

2-(4-Benzyloxyphenyl)-1-nitroethene (18)

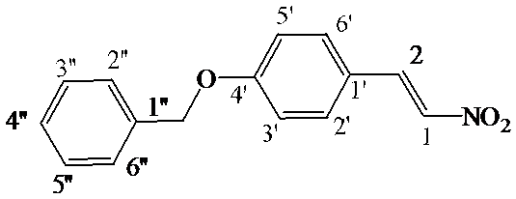

A solution of 4-benzyloxybenzaldehyde **17** (3.85 g, 18.2 mmol) and ammonium acetate (1.22 g, 15.8 mmol) in nitromethane (100 mL) was heated at 70 ˚C for 14 h. The cooled solution was diluted with CH_2Cl_2 (54 mL) and washed with saturated sodium chloride solution (200 mL), and distilled water (200 mL), dried over anhydrous magnesium sulfate, filtered and the solvent evaporated to dryness under reduced pressure. The crude product was recrystallized from ethanol (AR) to yield yellow needles (4.35 g, 94 %). Mp 114 – 115 ˚C, lit. (114 – 115 ˚C) (Rotich, 2010) IR: 3050 cm^{-1} (aliphatic C-H stretch), 1595 cm^{-1} (N=O), 1571 cm^{-1} (aliphatic C=C) stretch, 1340 cm^{-1} (N=O) stretch, ^{1}H NMR ($CDCl_3$, 200 MHz): δ 8.01 (1H, d, J = 13.2, H2), 7.94 (1H, d, J = 13.2 Hz, H1), 7.42 (5H, m, H2'', H3'', H4'', H5'' and H6''), 7.26 (2H, d, J = 8.6 Hz, H2', and H6'), 7.02 (2H, d, J = 8.6 Hz, H3' and H5') and 5.13 (2H, s, $ArCH_2O$). ^{13}C NMR ($CDCl_3$ 50 MHz): δ 162.3 (C-4'), 139.2 (C-1),

136.2 (C-2), 135.4 (C-1’’), 131.4 (C-2’, C-6’), 129.1 (C-2’’, C-6’’), 128.6 (C-4’’), 127.7 (C-3’’, C-5’’), 116.0 (C-3’, C-5’), and 70.5 ($ArCH_2O$.

2-(4-Benzyloxyphenyl)ethylamine (19)

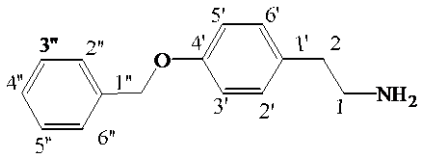

A solution of nitroethene **18** (1.00 g, 3.9 mmol) in 44 mL of THF was added drop wise over a period of 1 hour to a stirring and refluxing suspension of lithium aluminium hydride (0.59 g, 15.6 mmol) in THF (8.2 mL). The mixture was then refluxed for 4 h and then cooled to 0 ˚C. Saturated sodium sulfate solution was added cautiously to quench LAH and the mixture stirred for 30 more min. The white precipitate formed was filtered using a pad of Celite and the residue washed with large volumes of methanol. The filtrate was evaporated under reduced pressure and the brown crude product obtained was used in the next step without further purification.

***N*-[(2(4-benzyloxyphenyl)ethyl]-*tert*-butylcarbamate (20)**

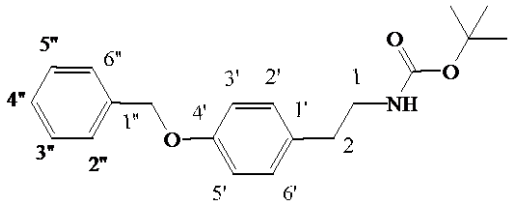

The mixture of amine **19** (0.88 g, 3.9 mmol) in acetonitrile (1.1 mL) and triethylamine (1 mL) was treated with di-*tert*-butyldicarbonate (2.56 g, 5.9 mmol) in acetonitrile (4.1 mL) at room temperature for 20 h. The solvent was evaporated in *vacuo* and the residual mass subjected to column chomatography employing 20 % ethylacetate in petroleum ether to yield colourless crystals in ethyl acetate (0.45 g, 27 %). Mp: 119 – 121 ˚C. IR: 3350 cm^{-1} (secondary NH), 2800 cm^{-1} (methyl C-H) stretch, and 1675 cm^{-1} (C=O). ^{1}H NMR ($CDCl_3$, 200MHz): δ 7.39 (3H, m, H3", H4" and H5"), 7.40 (2H, m, H6", H2"), 7.12 (2H, d, J = 8.6 Hz, H2’ and H6’), 6.93 (2H, d, J = 8.6 Hz, H3’ and H5’) and 5.05 (2H, s, $ArCH_2O$), 4.50 (1H, brs, NH), 3.35 (2H, t, J = 7.0 Hz, H1), 2.70 (2H, t, J = 7.0 Hz, H2) and 1.46 (9H, s, $OC(CH_3)_3$). ^{13}C NMR ($CDCl_3$ 50 MHz): δ 28.0 (CH_3), 79.3 ($OC(CH_3)_3$), 156 (C=O), 35.5 (C-2), 42.2 (C-1) 131.5 (C-1'), 130.0 (C-2', C-6'), 115.0 (C-3', C-5'), 158 (C-4'), 70.0 ($ArCH_2O$), 139 (C-1"), 127.5 (C-2", C-6"), 131.0 (C-3", C-5"), 128.0 (C-4").

***N*-[(2(4-hydroxyphenyl)ethyl]-*tert*-butylcarbamate (21)**

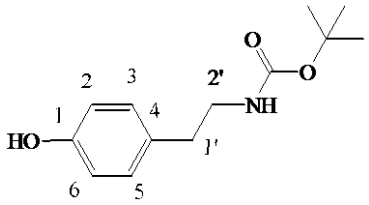

Hydrogen gas was bubbled into a flask containing a suspension of carbamate **20** (1.20 g, 3.7 mmol), 10% palladium-on-carbon (10 mol %) and ethanol (20 mL). The mixture was stirred at room temperature overnight. The product was filtered though a pad of Celite, washed with EtOAc (3x10 mL) and the filtrate concentrated under reduced pressure. The crude product was purified by column chomatography employing 20% EtOAc in petroleum ether to afford colourless crystals (0.5 g, 58 %). IR (KBr): ν_{max} 3600-3100 cm^{-1} (br) (OH), 2900 cm^{-1} (w), 1680 cm^{-1} (s) (CO), 1610 cm^{-1} (s) (C=C), 1505 cm^{-1} (s); ^{1}H NMR ($CDCl_3$, 200 MHz): δ 2.10 (2H, t, J = 7.0 Hz, H2'), 1.50 (2H, t, J = 7.0 Hz, H1'), 1.30 (9H, s, $OC(CH_3)_3$), 4.20 (1H, brs, NH), 7.40 (2H, d, J=8.4 Hz, H3, H5), 6.70 (2H, d, J = 8.4 Hz, H2, H6).

4-(2-Aminoethyl)phenol (22)

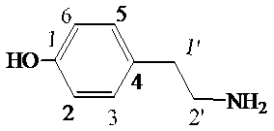

Trifluoroacetic acid (1mL) in CH_2Cl_2 (5 mL) was added drop wise to a solution of phenol carbamate **21** (0.12 g, 0.5 mmol) at 0 ºC and the mixture stirred for 30 min. Diisopropylethylamine (2 mL) was added and the solvent evaporated. The resultant amine was used in the next step without further purification.

***N*-(5-bromopyridin-2-yl)-1H-imidazole-1-carbothioamide (6)**

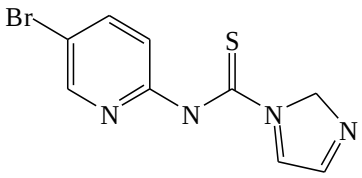

1,1-Thiocarbonyldiimidazole (4.12 g, 23.1 mmol) and 2-amino-5-bromopyridine (4.00 g, 23.1 mmol) was reacted in dry acetonitrile (22.5 mL) at room temperature. The reaction mixture was stirred for 12 h and the precipitate filtered, washed with cold acetonitrile. The resulting crude product was used in the next step without further purification.

***N*-[2-(4-Hydroxyphenyl)ethyl]-*N*'-[2-(5-bromopyridyl)]-thiourea (15)**

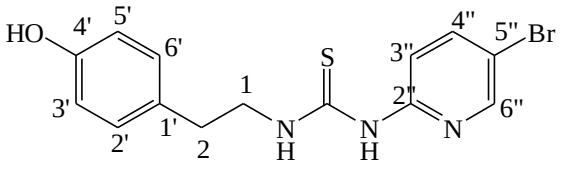

15

Thiocarbonyl derivative **6** (0.20 g, 0.6 mmol) was added to a solution of amine **22**, (0.12 g, 0.5 mmol) in 15 mL acetonitrile. The reaction mixture was stirred at room

temperature for 20 h. This was followed by evaporation of the solvent in the reaction mixture, and the crude product purified by column chomatography employing 30% ethylacetate in petroleum ether to furnish the titled compound as a pale yellow solid (0.10 g, 57%). Mp 165-167℃, IR: (KBr): 3350 cm^{-1} (OH), (br), 3200 (s) (N-H), 2900 cm^{-1} (s) (C-H), 1595 cm^{-1} (s) (C=C), 1525 cm^{-1} (s), 1460 cm^{-1} (s), 1235 cm^{-1} (w), 1240 cm^{-1} (m) (C-N), 1160 cm^{-1} (w) (C=S), 825 cm^{-1} (w) (N-H); ^{1}H NMR ($CDCl_3$, 200 MHz): δ 3.08 (H1, d, J = 7.2 Hz), 3.00 (H2, d, J = 7.2Hz), 7.06 (H2', H6', d, J = 8.4 Hz) 6.77 (H3', H5', d, J = 8.4 Hz), 7.10 (H3'', d, J=8.0 Hz), 7.52 (H4'', d), 7.79 (H6'', s), 8.88 (1H, brs, NH), 11.18 (1H, brs, NH). 13C NMR (CDCl3 50 MHz): δ 132.3 (C-2', C-6'), 115.8 (C-3', C-5'), 155.7 (C-4'), 132.6 (C-1'), 47.7 (C-1), 34.14 (C-2), 179.3 (C=S), 151.9 (C-2''), 113.0 (C-3''), 146.7 (C-4''), 106.4 (C-5''), 154.7 (C-6'').

3.2 Docking aspects

The structure of the target compound **15** was drawn using Chemsketch and converted to pdb using Avogadro software. The binding conformations of **15** bound to HIV-1 Reverse Transcriptase (RT) were modeled using AutoDock 4.2 (pdb file number 3ITH). Polar hydrogen atoms were added to the peptide and Kollman united-atom partial charges allocated using the AutoDock-Tools package. Gasteiger-Marsili partial charges were assigned, as executed in AutoDockTools. Electrostatic contacts were calculated using a distance-dependent dielectric constant. Atomic solvation parameters and fragmental volumes were assigned via the AddSol utility, from which the desolvation contribution to the binding free energy was calculated. All docking calculations were done using a 61 _ 61 _ 61 grid map, with a grid spacing of 0.375 Å. Since the position of the NNIBP is known, the grid was positioned on the coordinates

for the corresponding atom of PETT-ligand, equivalent to the default selected root atom of the ligand.

The Lamarckian genetic algorithm (LGA) was used to generate docked conformations. Other parameters were set to their default values. A total of 10 runs were performed and the resulting conformations clustered using a root mean-square deviation criterion of 0.5 Å in x, y, z positional coordinates. Rotation of the pyridinyl ring along the C-N (thiourea) was prohibited, while the conformation was set to accommodate the known intramolecular hydrogen bond between the hydrogen of one of the thiourea nitrogens and the nitrogen of the pyridinyl ring (D'Cruz and Uckun, 2005) to form a flat six-membered pseudo-ring (Hunter *et al.,* 2008). Visualization was done using Python Molecule View (PMV).

3.3 X-ray Analysis

3.3.1 Preparation and Selection of Single Crystals

N-[(2(4-benzyloxyphenyl)ethyl]-*tert*-butylcarbamate, **21** was recrystallized from ethanol at room temperature. Good quality single crystals were selected and the crystal faces checked using the phase contrast microscope (Fig 3.1).

Fig 3.1: Phase contrast microscope (Rotich, 2010)

3.3.2 X-ray Crystal Structure Analysis

To determine the crystal structure of *N*-[(2(4-benzyloxyphenyl)ethyl]-*tert*-butylcarbamate (21**)**, X-ray diffraction data were collected at 100 K using *CrysAlis CCD* Gemini (molybdenum source) and SuperNova (copper source) X-ray diffractometers. The X-ray data collection parameters were as follows: 1.54180 Å wavelength, 55 mm detector distance, generator settings; 50KV, 1mA, 1.5/3.5 second exposure times (low/high angle), 1 degree scan width, 10 omega scans, 639 total frames and the total data collection time of 1h 24 minutes. The SuperNova X-ray diffractometer used very short exposure times compared to the Gemini and the overall

experiment time was 8 hours faster. The cell refinement was carried out using *CrysAlis CCD* and data reduction was done using *CrysAlis RED*. The lower intensity Cu Ultra gave slightly better structural refinement results as data collection time was cut short on the SuperNova Microfocus Cu source. *SHELXS97* was used to solve and refine structures and molecular graphics done using ORTEP-3 of Mercury version 3.0 software.

CHAPTER FOUR

RESULTS AND DISCUSSION

4.1 Syntheses

A thiourea derivative *N*-[2-(4-hydroxyphenyl)ethyl]-*N*'-[2-(5-bromopyridyl)]-thiourea **15** was the target compound for this synthesis (Fig 4.1).

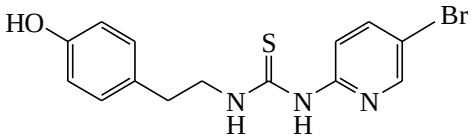

15

Fig 4.1: Structure of target molecule for this synthesis

The retrosynthetic analysis of **15** (Scheme 4.1) could be envisioned to proceed via two possible routes, depending on the timing of introduction of the thiourea moiety. Route **a** involved coupling amine **19** with thiourea derivative **6** to afford **23** which would then undergo catalytic hydrogenolysis in a debenzylation reaction to give the desired target compound **15**. Although this route had fewer steps, it posed a foreseen problematic debezylation, in view of a possible 'poisoning' of the catalyst by the thiocabonyl group. The second route **b** had more steps as a result of Boc protection of the amine before the ultimate incorporation of the thiourea moiety. This was deemed more feasible, since it was easier to purify the intermediate products and posed no chemoselectivity problems during debenzylation.

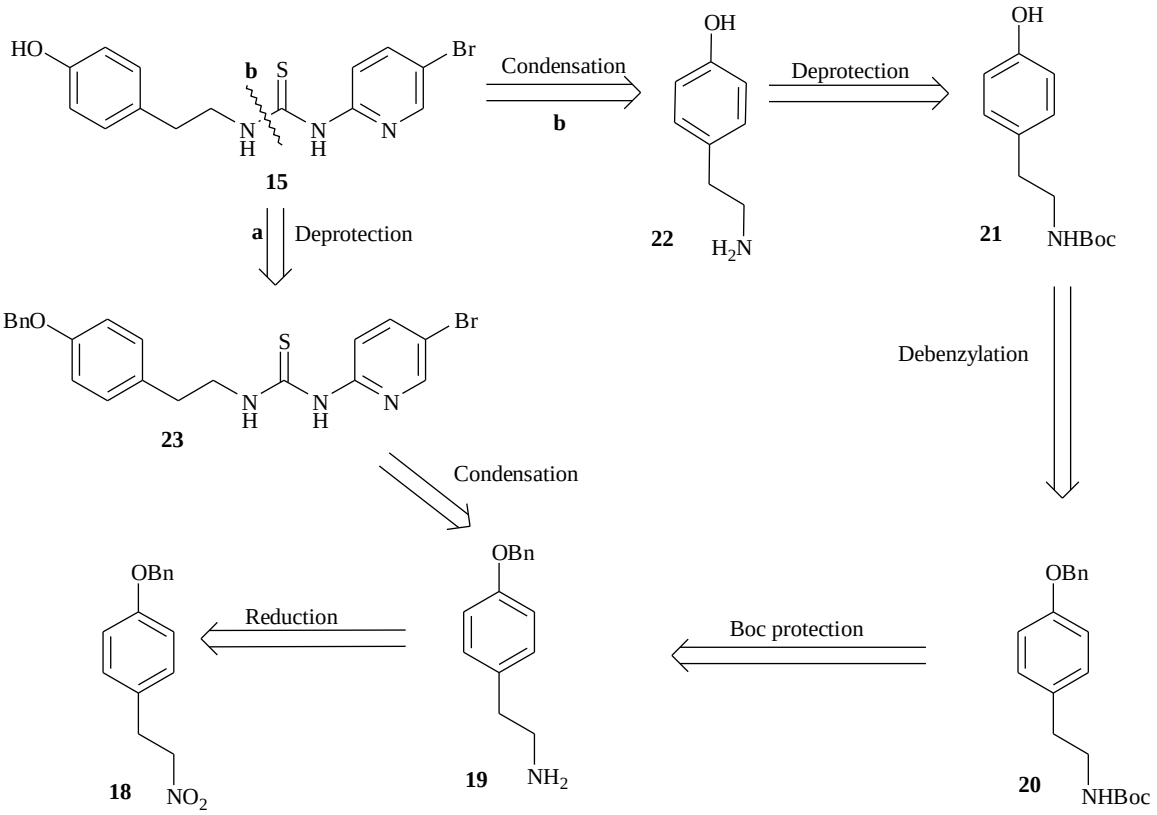

Scheme 4.1: A retrosynthetic analysis of the target molecule

The actual synthesis of the target compound began with a three step reaction series as developed by Glennon *et al*., (1980) and modified by Younis *et al.*, (2010). The reaction sequence commenced with the phenolic hydroxyl group protection of the commercially available reagent **16** by benzylation into its benzyl ether **17,** using benzyl bromide and anhydrous potassium carbonate as a base in ethanol at reflux for 1

h, to afford colourless needles of 4-benzyloxybenzaldehyde **17** (Fig 4.2)**,** with a yield of 95% (scheme 4.2).

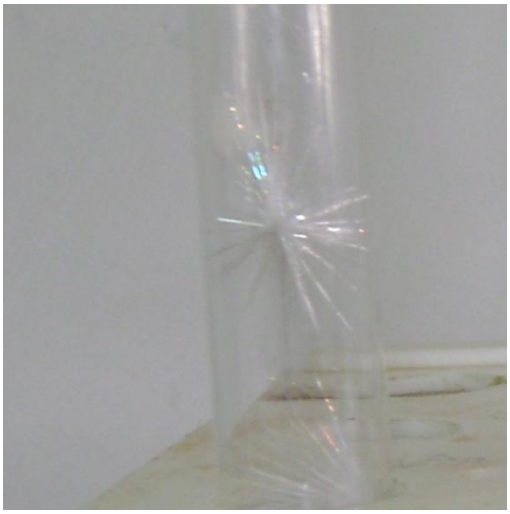

Fig 4.2: Colourless needles of 4-benzyloxybenzaldehyde in a test-tube (Author)

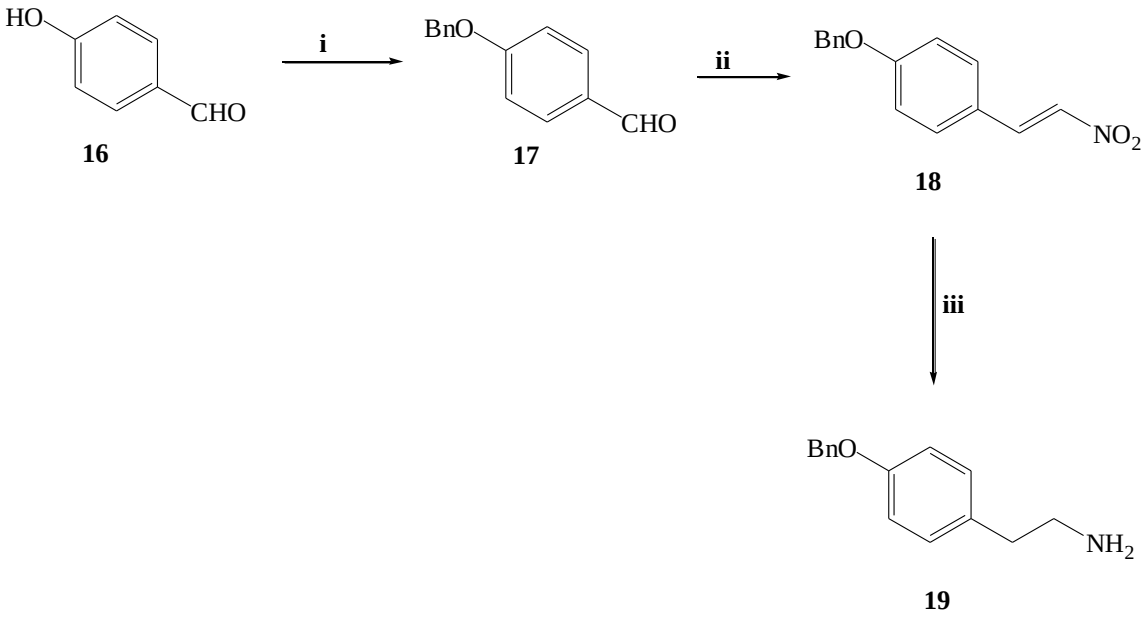

Scheme 4.2: *Reagents and conditions* (i) BnBr, K_2CO_3, EtOH, reflux, 3 h, 95 % yield. (ii) CH_3NO_2, NH_4OAc, 70 ˚C, 14 h, 94 %. (iii) LAH, THF, 4 h.

Its melting point was found to be 71-74 ˚C, which is in agreement with literature value of 71 – 74 ˚C (Rotich, 2010). Furthermore, the success of the benzylation process was corroborated by the spectroscopic data. ^{1}H NMR spectrum of compound **17** displayed signals at δ_H 5.13 for the benzylic methylene protons as well as aromatic signals at 7.42 (5H). Its ^{13}C NMR spectrum, exhibited a diagnostic peak at δ_C 70.5 for the $ArCH_2O$ of the benzyl group. Its IR spectrum further revealed the presence of an ether (C-O-C) at 1260 cm^{-1} as well as the absence of an -OH broad band between 3300-3600 cm^{-1}, an indication of successful benzylation. Mechanistically, the presence of potassium carbonate as a base resulted to the abstraction of a proton on compound **16**, forming a phenoxide ion. This highly

nucleophilic species then attacks benzyl bromide in an S_N2 fashion, leading to the formation of 4-benzyloxybenzaldehyde (Fig 4.3).

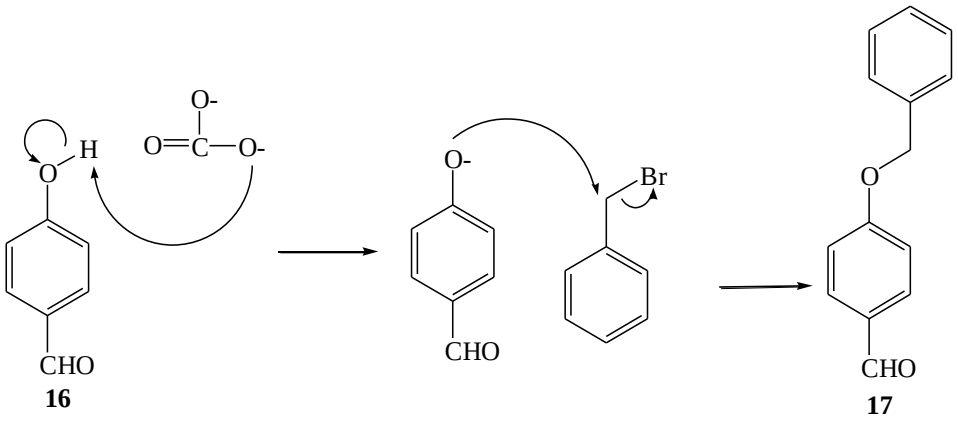

Fig 4.3: Mechanism for the formation of 4-benzyloxybenzaldehyde

Aldehyde **17** was then reacted with nitromethane in a Henry-Aldol condensation (Basavapathuni *et al*., 2004) in the presence of ammonium acetate as a base at 70 ˚C to afford nitrostyrene, compound **18** in 94% yield as yellow needles. Its melting point of 114-115 °C was in agreement with the literature value of 114-115 °C (Rotich, 2010). The assignment of the structure was also supported by its IR spectrum which displayed N=O peaks at 1595 cm^{-1} and 1340 cm^{-1}. Its ^1H NMR spectrum displayed no peaks at δ_H 10.51 showing the absence of an aldehyde group (CHO), with the emergence of new signals at δ_H 8.01 and δ_H 7.94 for H2 and H1 respectively. Supplementary evidence for the formation of **18** was shown by its ^{13}C NMR spectrum

that displayed new signals at δ_C 139.2 (C-1) and δ_C 136.2 (C-2) in addition to the absence of aldehydic peak at δ_C 190.0.

The mechanism of this reaction commenced with the base abstraction of acidic protons in nitromethane by the acetate anion. Subsequent nucleophilic attack on the carbonyl carbon of the aldehyde led to the formation of the nitro alcohol. Following this was an *E-1cB* elimination of water to give 4-benzyloxynitrostyrene **18** (Fig 4.4)**.**

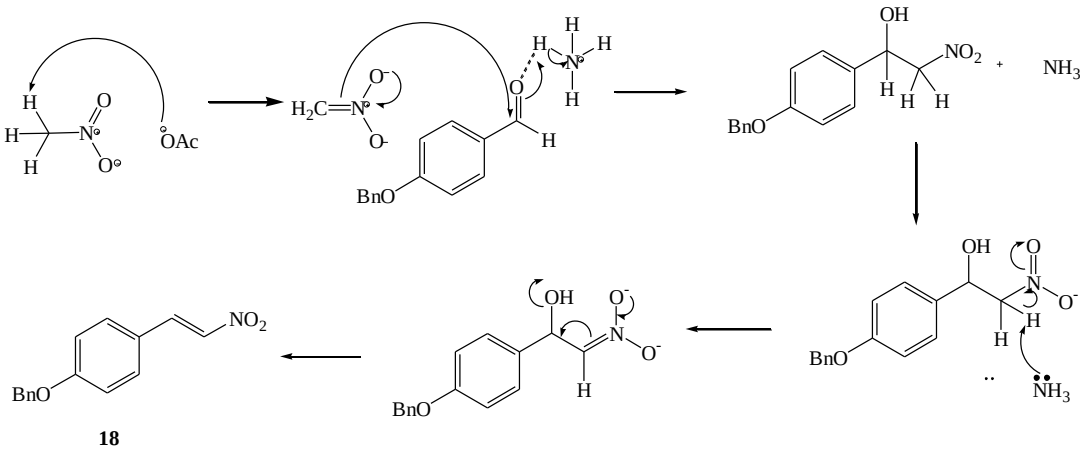

Fig 4.4: Mechanism of formation of compound 18**.**

In the next step, nitrostyrene **18** was transformed into amine **19** in a LAH reduction in THF at reflux for four hours. The crude amine was used in the next step without purification due to its expected high polarity and nucleophilicity. The amine functionality of **19** was Boc protected to give the desired carbamate **20** (scheme 4.3). This was achieved by treating a mixture of the amine and triethylamine in acetonitrile with di-*tert*-butyldicarbonate at room temperature for 20 hours to furnish colorless crystals of compound **20** in 26% yield. The ^{1}H NMR spectrum of **20** revealed the presence of a methyl singlet at δ 1.44, and a downfield shift in the methylene protons

adjacent to nitrogen at δ 3.34 (Fig. 4.5 (a-b)). Its ^{13}C NMR spectrum displayed the presence of a carbamate carbonyl carbon at δ 156.1 and a methyl carbon at δ 28.6.

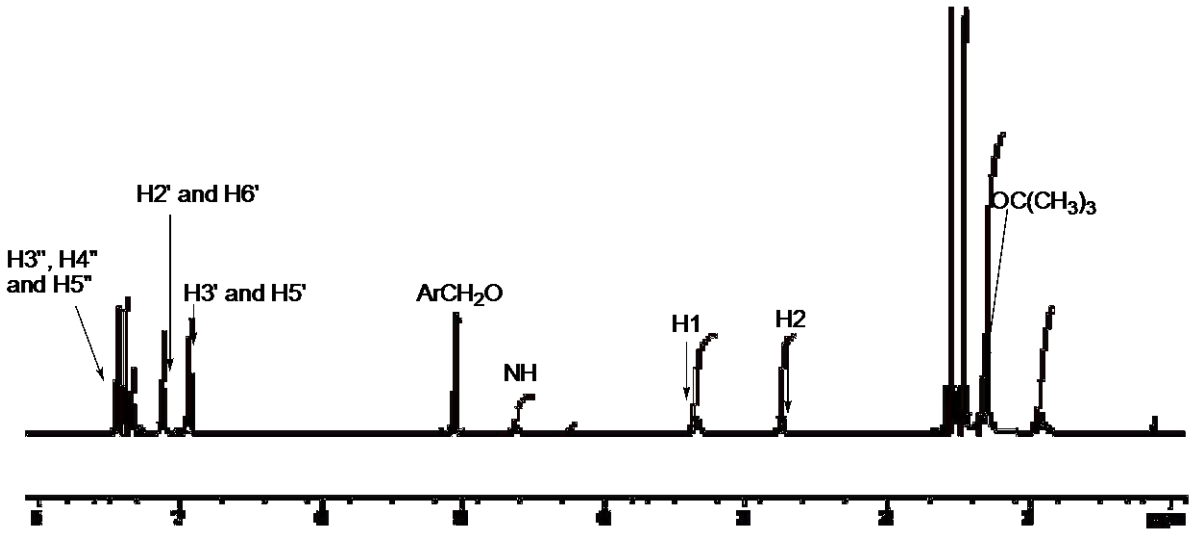

Fig 4.5 (a): ^{1}H NMR spectrum of 20.

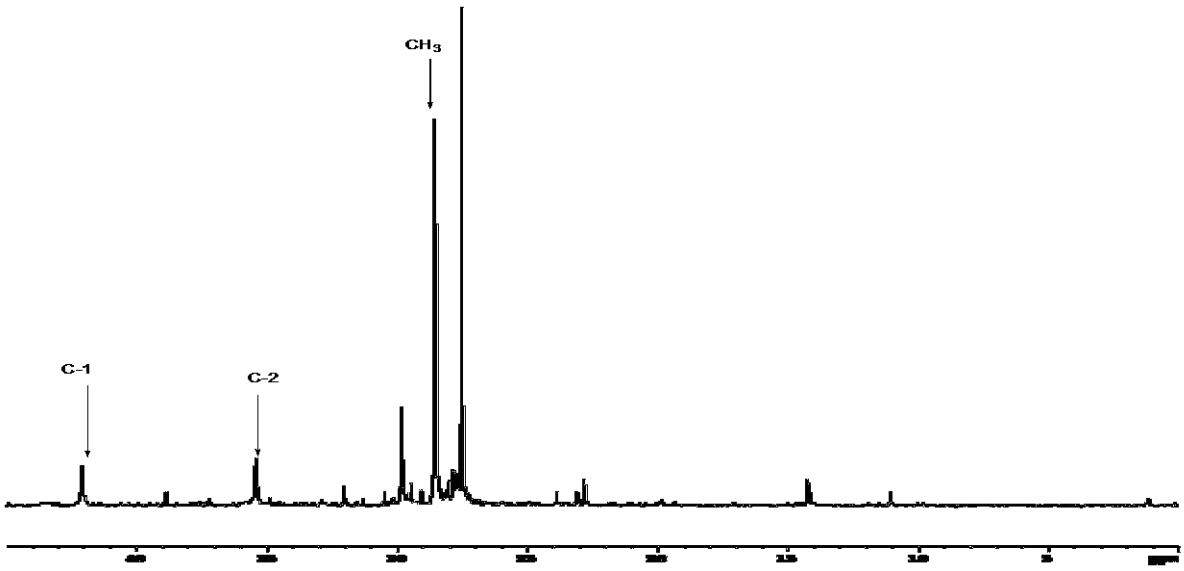

Fig 4.5 (b): ^{13}C NMR spectrum of 20.

In this reaction, the nucleophilic amine attacks di-*tert*-butyldicarbonate directly to form the Boc-protected amine **20** (Fig. 4.6).

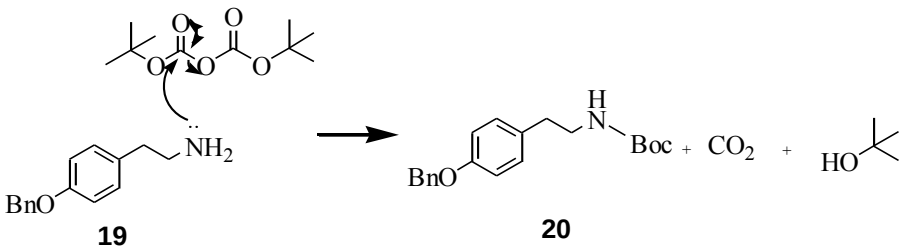

Fig 4.6: Mechanism of formation of compound 20.

The next step involved debenzylation of compound **20** by hydrogenolysis in the presence of 10% palladium-on-carbon in ethanol at room temperature to furnish

phenol **21.** An early indication of successful reaction was a lower R_f value (0.35) of the product on TLC as compared to the reactant (0.53).

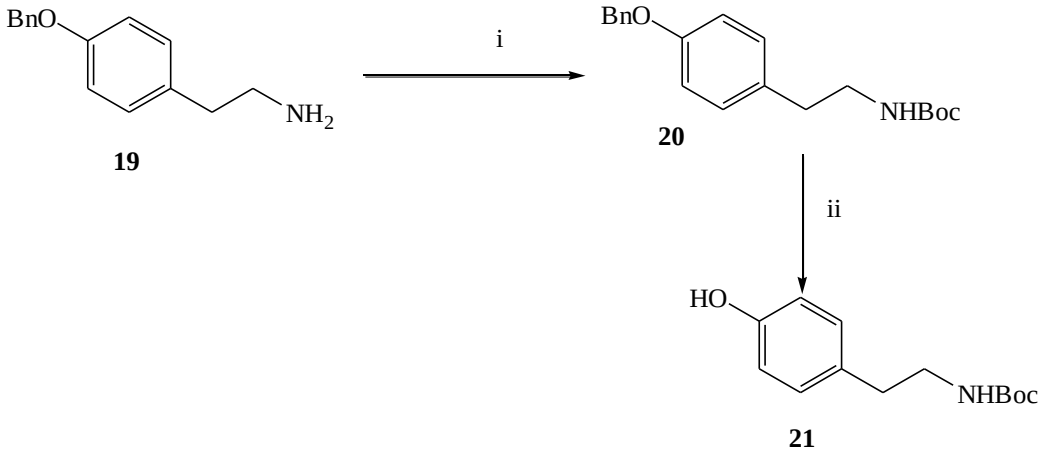

Scheme 4.3: *Reagents and conditions*; (i) $(Boc)_2$, Et_3N, CH_3CN, rt, 20 h, 27 % yield. (ii) H_2, Pd/C, EtOH, rt, 12 h, 58 % yield.

This was verified by its IR spectrum which revealed the presence of a broad peak at 3600-3100 cm^{-1} for the hydroxyl stretch. Its ^1H NMR spectrum revealed the absence of a benzylic methylene singlet at δ 5.05 (Fig 4.7).

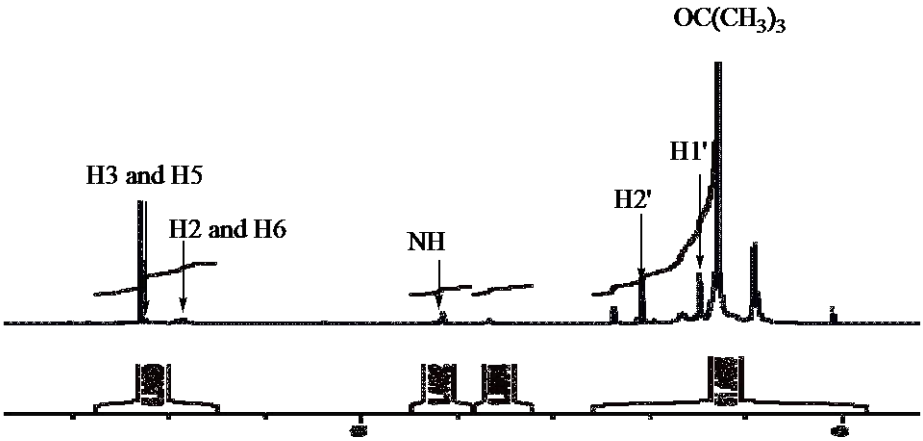

Fig 4.7: ^{1}H NMR spectrum for phenol 21.

The required target thiourea derivative **15** was prepared starting from phenol carbamate (2**1**), through aminophenol **22** as a key intermediate for the final coupling reaction in a *one-pot* sequential reaction strategy (Scheme 4.3). In the first step, **21** was treated with trifluoroacetic acid in dichloromethane at 0 ^{o}C for 30 minutes, followed by diisopropylethylamine to furnish a brown oily amine **22**, which was extracted and used without further purification.

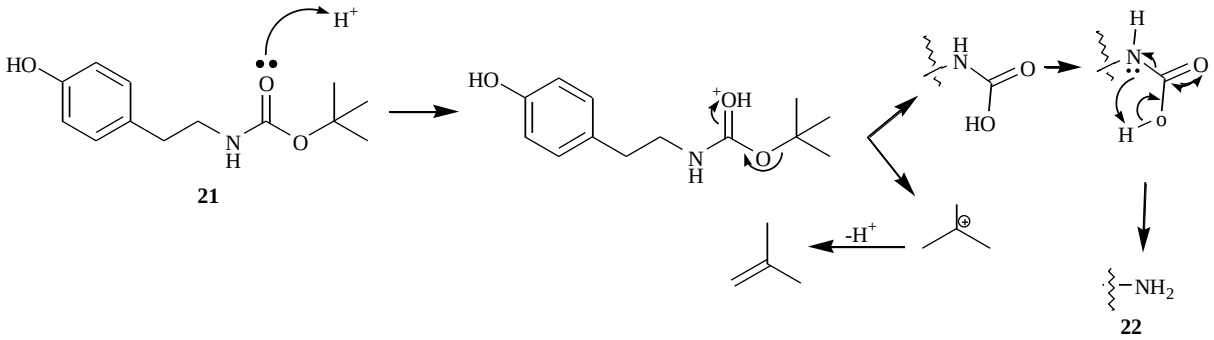

Fig 4.8: Mechanism of Boc deprotection

The mechanism of this reaction involved protonation of the carbonyl oxygen to yield carbamic acid with the elimination of *tert*-butyl cation. The acid was then decarboxylated to form amine **22** (Fig 4.8).

Synthesis of the target compound **15**, was preceded by the condensation of 2-amino-5-bromopyridine with 1,1'-thiocarbonyldiimidazole in acetonitrile at room temperature for 12 h, according to literature (Hogberg *et al.*, 2000) (Scheme 2.3). The precipitate **6** formed, was used without purification in anticipation of its poor stability towards nucleophilic attacks. Amine **22** was then treated with **6** in a nucleophilic coupling reaction to give the target compound **15** (Scheme 4.4) as a pale yellow solid in 57% yield (after column chromatography). The spectroscopic data of **15** were in complete agreement with the assigned structure. Its IR spectrum exhibited a broad band at 3350 cm^{-1} for the OH, as well as

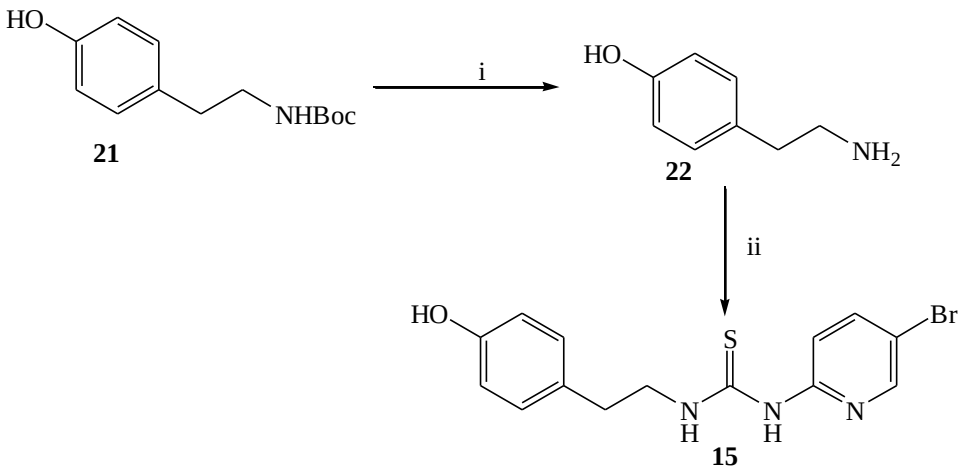

Scheme 4.4: *Reagents and conditions*: (**i**) CF_3COOH, CH_2Cl_2, 0 ˚C, 30 min. (**ii**) THF, 6, 12 h, 57 %.

the C=S stretch at 1160 cm^{-1}. This was also confirmed by its ^{1}H NMR spectrum which displayed resonances for the diagnostic thiourea NH protons at δ 11.18 and δ 8.88 whereas, its ^{13}C NMR spectrum showed the presence of a thiocarbonyl carbon at δ 179.3 (Fig 4.9 (a) and Fig 4.9 (b)).

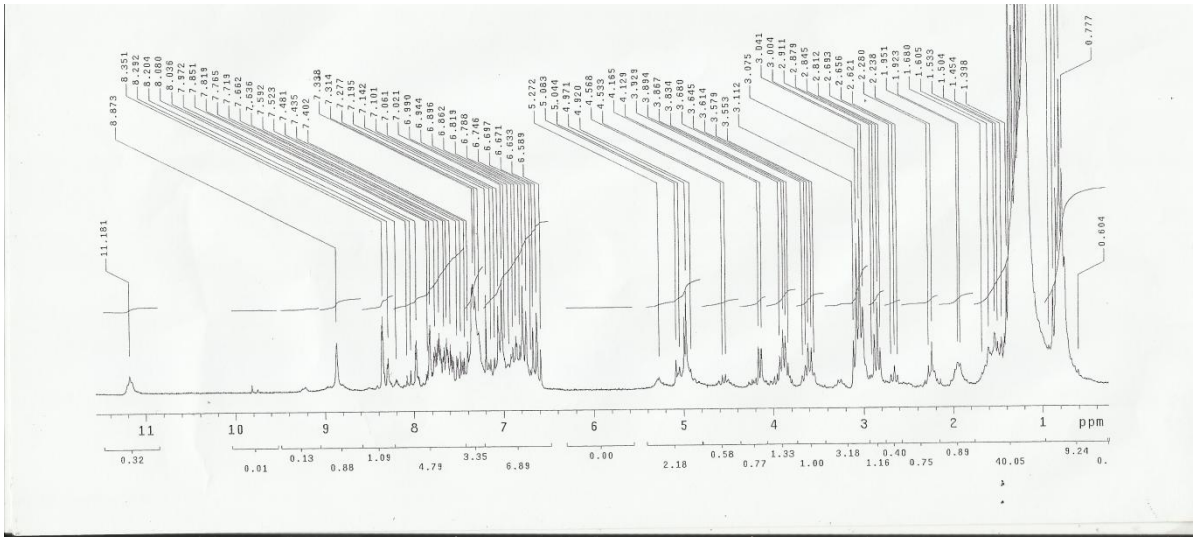

Fig 4.9 (a): ^{1}H NMR spectrum for 15.

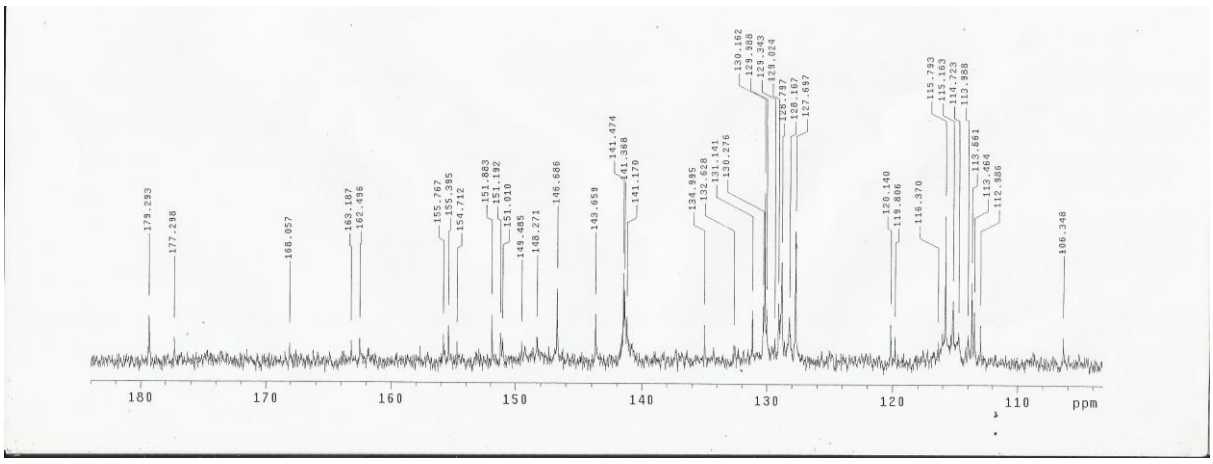

Fig 4.9 (b): Expanded ^{13}C NMR spectrum for 15.

A search for the three compounds, **15**, **21**and **22** using available web based search engines reveals that they are unknown. This indicates that they are new compounds and therefore have never been synthesized. However, **15** displayed more NMR peaks than expected, owing to the presence of impurities in the sample. Efforts made to improve on the sample purity by column chromatography and recrystallization led to the decrease of sample amounts below the minimum quantities (less than 5 mg) needed for characterization by NMR analysis at 200 MHz.

4.2 Modeling studies

In order to investigate the possible binding and interaction mode of the synthesized compound with RT, **15** was docked into the NNIBP in the most energetically favourable conformation (Fig 4.10), and interacted with amino acid residues of the RT allosteric pocket. The compound displayed an estimated free binding energy of -7.50 kcal/mol, which is a revelation that it had fairly strong interactions with NNIBP. This compares favourably with dapivirine which exhibited a free binding energy of -7.97 kcal/mol (Liang and Chen, 2007). This high stability of the enzyme/inhibitor complex may be attributed to the strong interactions via H-bonds of a thiocarbonyl group (C=S) and amino hydrogen of the Lys 101 side chain. Moreover, the phenyl ring exhibits strong π-π stacking contacts with the two aromatic rings of Tyr 181 and Tyr 188. Similar connections between the inhibitor and RT have been shown by other NNRTIs like Efavirenz and Nevirapine (Kuno *et al.*, 2003 and Nunrium *et al*., 2005). The estimated inhibition constant, K_i was found to be 3.18 µM [Temperature = 298.15

K], which is one and a half times more active than the first NNRTI, HEPT whose IC_{50} is 5 µM (Miyasaka *et al.,* 1989). It is however less active compared to the conventional NNRTIs like Delavirdine (0.009 µM) and Nevirapine (0.03 µM) (Venkatachalam *et al.,* 2004).

.

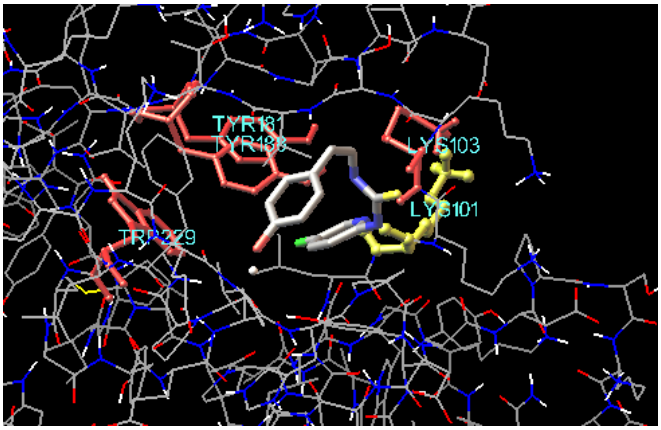

Fig 4.10: The target molecule (15) in the NNIBP

4.3 X-ray analysis of *N*-[(2(4-benzyloxyphenyl)ethyl]-*tert*-butylcarbamate

Single crystal X-ray diffraction for *N*-[(2(4-benzyloxyphenyl)ethyl]-*tert*-butylcarbamate (**21**) gave further confirmation that this compound was successfully synthesized. Its empirical formula agreed well with the expected formula (C_{20} H_{25} N O_3) and the observed molecular weight of 327.41 was also in concurrence with the theoretical value of 327.42. This implies that **21** exists as a monomer, unlike **18**, which is trimeric (Kennedy *et al.,* 2010[b]). The compound has a monoclinic crystal system with a space group of P21/c. Its unit cell parameters were: a = 11.040(3) Å, b = 5.0931(12) Å, c = 64.070(16) Å, α= 90°, β= 94.493(14)°, γ = 90°, Z=8 and cell volume 3591.4(16) $Å^3$ (Table 4.1).

Table 4.1: Crystal data and structure refinement for *N*-[(2(4-benzyloxyphenyl)ethyl]-*tert*-butylcarbamate (21)

Property	Parameter
Empirical formula	C_{20} $H_{25}N$ O_3
Formula weight	327.41
Temperature	100(2) K
Wavelength	1.54180 Å
Crystal system	Monoclinic
Space group	$P2_1/c$
Unit cell dimensions	a = 11.040(3) Å α= 90° b = 5.0931(12) Å β= 94.493(14)° c = 64.070(16) Å γ = 90°
Volume	3591.4(16) $Å^3$
Z	8

The crystal structure of this compound as obtained from the X-ray structure solution (Fig. 4.11) was also in agreement with the assigned structure (Scheme 4.3).

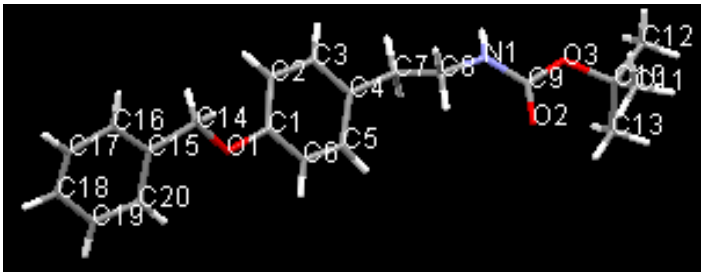

Fig 4.11: (a) A capped stick X-ray skeletal structure of a compound with non-Hydrogen atomic labels

Eight molecules of the crystals of this compound were packed in one unit cell (Z=8). The observed unit cell parameters were a = 11.4772(11)Å (α = 90.0°), b = 12.9996(12) Å, (β = 90.0°) and c = 7.2032(6) Å (γ = 90.0°) and cell volume 3591.4(16) $Å^3$ (Table 4.1).

The molecules arrange themselves in pairs with each pair oriented in a particular direction within a given line and an opposite orientation is observed in the neighbouring pair of molecules (Fig. 4.12).

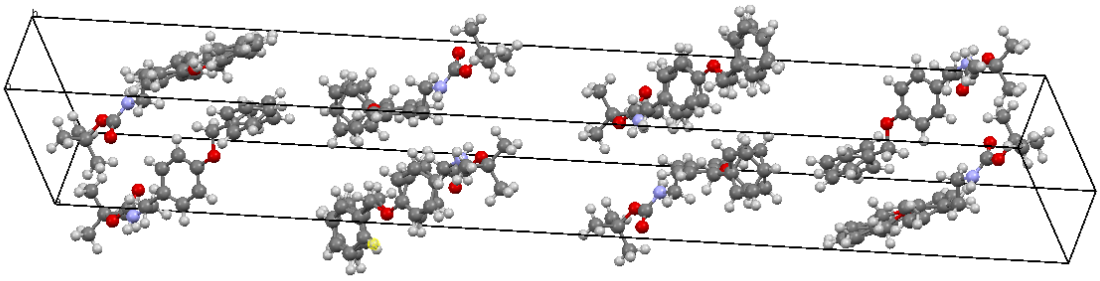

Fig 4.12: Molecular packing in the crystals of *N*-[(2(4-benzyloxyphenyl)ethyl]-tert-butylcarbamate

This well-organized packing pointed out to the existence of ordered bonding between the molecules. Crystals of **20**, were found to exist in discrete monomeric molecules held by some intermolecular forces such as hydrogen bonds, N—H···O=C interactions involving carbonyl O atom and amine H atom (H···O =2.14 Å) (Fig. 4.13(a)). Additionally, there were non classical hydrogen bond C-H···O=C interactions involving aromatic H and carbonyl O atoms (H···O = 2.80 Å) as well as van der waals forces (Fig 4.13(b)).

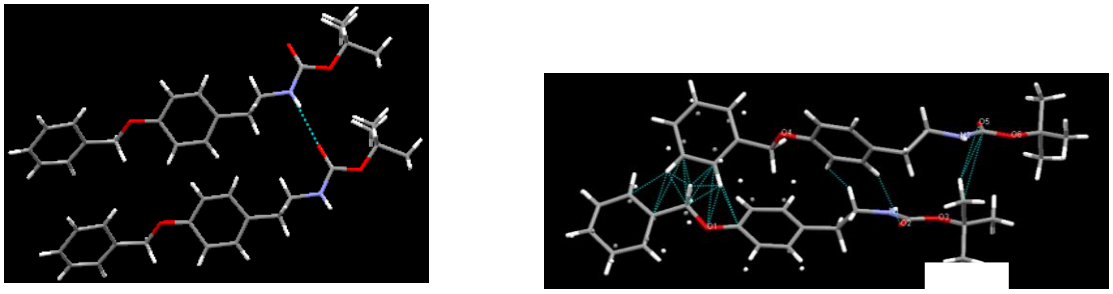

a b

Fig 4.13: (a) A pair of molecules held together by H-bond. (b) The molecules with additional intermolecular interactions.

Similar interactions have been described by Gerkin (1999). Bond lengths were similar to those found in the structures of related compounds. Unlike the earlier intermediate, 4-benzyloxybenzaldehyde, the benzyl and the phenyl rings were not coplanar to each other (C16, C20, C2 and C6 = -15.8 (3) °). Similarly, substituted species described by Gerkin (1999), Allwood *et al*. (1985) and Liu *et al*., (2007) were also, twisted with torsion angles ranging from 31.7 to 99.1°. The other refinement details for *N*-[(2(4-

benzyloxyphenyl)ethyl]-*tert*-butylcarbamate such as atomic coordinates, bond lengths and torsion angles are given in the Appendix.

CHAPTER FIVE

CONCLUSION AND RECOMMENDATIONS

5.1 CONCLUSION

In this research, three new compounds **15, 21** and **22** were synthesized. Carbamate **21** was formed by hydrogenolytic debenzylation of **20** at room temperature for 12 hours. Subsequent Boc deprotection of the carbamate, followed by a condensation reaction with thiourea derivative **6** furnished the target compound **15**, as a pale yellow solid in 57 % yield. Molecular modeling studies were

done to provide an insight into the mode of interaction of this ligand with its active site. The enzyme–inhibitor complex displayed an estimated free binding energy of -7.50 kcal/mol, which is a revelation that it had fairly strong interactions with NNIBP. This high stability of the enzyme-inhibitor complex was attributed to the strong interactions via H-bonds of a thiocarbonyl group (C=S) and amino hydrogen of the Lys 101 side chain. Additionally, the phenyl ring exhibited strong π-π stacking contacts with the two aromatic rings of Tyr 181 and Tyr 188. The estimated inhibition constant, $K_{i,}$ was found to be 3.18 µM [temperature = 298.15 K]. Single crystal X-ray diffraction analysis for *N*-[(2(4-benzyloxy- phenyl)ethyl]-*tert*-butylcarbamate **21** crystals revealed that its molecular weight is 327.41. This compound was found to exist in discrete monomeric molecules. It has a monoclinic crystal system with a space group of P21/c and each unit cell contains eight molecules of the compound (Z=8). The observed regular packing was attributed to the existence of ordered intermolecular forces between the molecules such as hydrogen bonds due to N—

H···O=C interactions involving the carbonyl O atom and amine H atom (H···O =2.14 Å). Other interparticle forces exposed include non-classical hydrogen bond (C-H···O=C) interactions involving aromatic H and carbonyl O atoms (H···O = 2.80 Å) as well as van der waals interactions.

5.2 RECOMMENDATIONS

Future work should involve:

- Biological testing of **15** to ascertain its anti-HIV activity.
- Structure activity relationship (SAR) studies and synthesis of a library of compounds, comprising of various substitutions of the hydrogen on the hydroxyl group of the target compound, should be done in order to increase the chances of discovering a superior NNRTI.
- Crystallographic studies need to be done on compounds **15** and **21** for a deeper insight of their solid state properties.

REFERENCES

Allwood, B. L., Kohnke, F. H., Slawin, A. M. Z., Stoddart, J. F. and Williams, D. J. (1985). "An Adduct Between Tetraammine(1,10-phenanthroline)ruthenium(II) and Dibenzo-42-crown-14." *Chem. Commun.*, 311–314.

Baba, M., Tanaka, H., De Clercq, E., Pauwels, R., Balzarini, J., Schols, D., Nakashima, H., Perno, C. F., Walker, R. T. and Miyasaka, T. (1989). "Highly specific inhibition of human immunodeficiency virus type 1 by a novel 6-substituted acyclouridine derivate." *Biochem. Biophys. Res. Commun*., **165**: 1375–1381.

Balzarini, J. (2004). "Current status of the non-nucleoside reverse transcriptase Inhibitors of human immunodeficiency virus type 1." *Curr. Top. Med. Chem*., **4**: 921-944.

Basavapathuni, A., Bailey C. M., Anderson K. S. (2004) "Defining a molecular mechanism of Synergy between nucleoside and nonnucleoside AIDS drugs". *J. Biol. Chem.* 20; 279(8):6221-6224.

Bell, F. W., Cantrell, A. S., Hogberg, M., Jaskunas, S. R., Johansson, N. G., Jordan, C. L., Kinnick M. D., Lind, P., Mori, Jr. M., Noreen, M. R. and Huang, L. J. (1995). "Phenethylthiazolylthiourea (PETT) compounds, a new class of HIV-1 Reverse Transcriptase Inhibitors. 1. Synthesis and basic structure–activity relationship studies of PETT analogs." *J. Med Chem.*, **38**: 4929-36.

Bryce, R. M., Finn, T., Moore, J.A., Batsanov, S. A., and Howard, A. K. J. (2000). "Synthesis and X-ray crystal structure of functionalized 9,10-Bis(1,3 dithiol-2-ylidene)-9, 10-dihydroanthracene derivatives)." *Eur. J. Org. Chem.*, 51 – 60.

Cantrell, A. S., Engelhardt, P., Hogberg, M., Jaskunas, S. R., Johansson, N. G., Jordan, C. L., Kangasmetsa, J., Kinnick, M. D., Lind, P., Morin, J .M., Jr, Muesing, M. A., Noreen, R., Oberg, B., Pranc, P., Sahlberg, C., Temansky, R. J., Vasileff, R. T., Vrang, L., West, S. J. and Zhang, H. (1996). "Phenethylthiazolylthiourea (PETT) compounds as a new class of HIV-1 reverse transcriptase inhibitors. 2. Synthesis and further structure-activity relationship studies of PETT analogs." *J. Med. Chem.*, **39**: 4261-4274.

Carr, A. (2003) "Toxicity of antiretroviral therapy and implications for drug development" *Nat. Rev Drug Discover.*, **2**: 624–634.

Christer, S., Rolf N., Per E., Marita H., Jusii K., Lotta V. and Hong, Z. (1998). "Sythesis and anti-HIV activities of Urea-PETT Analogs Belonging to a new class of Potent Non- Nucleoside HIV-1 Reverse Transcriptase Inhibitors." *Bioorg. Med. Chem. lett.*, **8**: 1511-1516.

Cooley, L. A. and Lewin, S. R. (2003). "HIV-1 cell entry and advances in viral entry inhibitor therapy." *J.Clin. Vir.*, **26**: 121-132.

D'Cruz, O. J. and Uckun, F. M. (2005). "Discovery of 2,5-dimethoxy-substituted 5-bromopyridyl thiourea (PHI-236) as a potent broad-spectrum anti-human immunodeficiency virus microbicide." *MH: Basic Sci. of Reprod. Med.*, **11**: 767-777.

Daelemans, D., Dumont, J., Rosenwirth, B., De Clercq, E. and Pannecouque, C. (2010). "Debio-025 Inhibits HIV-1 by interfering with an early event in thereplication cycle." *Antivir. Res*., **85**: 418-421.

Das, K., Lewi, P. J., Hughes, S. H. and Arnold, E. (2005). **"**Crystallography and the design of anti-AIDS drugs: Conformational flexibility and positional adaptability are important in the design of non-nucleoside HIV-1 reverse transcriptase inhibitors." *Progr. Biophys. Mol .Biol*., **88**: 209-231.

de Béthune, M. P. (2010). "Non-nucleoside reverse transcriptase inhibitors (NNRTIs), their discovery, development, and use in the treatment of HIV-1 infection: A review of the last 20 years (1989-2009)." *Antivir. Res*., **85**: 75-90.

De Clercq, E. (2009). "Another ten stories in antiviral drug discovery (part C): "old" and "new" antivirals, strategies, and perspectives." *Med. Res. Rev*., **29**: 611-645.

De Clercq, E. (2010 [a]). "In search of a selective therapy of viral infections." *Antivir. Res.*, **85**: 19-24.

De Clercq, E. (2010[b]). "Antiretroviral drugs." *Curr. Opin. Pharmacol.*, **10**: 1-9.

De Corte, B. L. (2005). "From 4,5,6,7-tetrahydro-5-methylimidazo[4,5,1-jk](1,4)benzo- diazepin-2(1H)-one (TIBO) to etravirine (TMC125): fifteen years of research on non-nucleoside inhibitors of HIV-1 reverse transcriptase." *J. Med. Chem*., **48**: 1689−1696.

Debyser, Z., Pauwels, R., Andries, K., Desmyter, J., Kukla, M., Janssen, P.A. and DeClercq, E. (1991). "An antiviral target on reverse transcriptase of human immunodeficiency virus type 1 revealed by tetrahydroimidazo-[4,5,1-jk]

[1,4]benzodiazepin-2-(1H)-one and -thione derivatives." *Proc. Natl. Acad. Sci*., **88**: 1451-1455.

Ding, J., Das, K., Moereels, H., Koymans L., Andries, K., Janssen, P. A., Hughes, S. H. and Arnold, E. (1995). "Structure of HIV-1 RT/TIBO R 86183 complex reveals similarity in the binding of diverse nonnucleoside inhibitors." *Nat. Struct. Biol*., **2**: 407−415.

Douek, D. C., Roederer, M. and Koup, R. A. (2009). "Emerging concepts in the immunopathogenesis of AIDS." *Annu. Rev. Med.*, **60**: 471-84.

Gerkin, R. E. (1999). "Network of C-H...O interactions in 4-benzyloxy-3-methoxybenzaldehyde (vanillin benzyl ether)." *Acta Cryst*., 55: 2140–2142.

Glennon, R. A., Liebowitz, S. M., Leming-Doot, D. and Rosecrans, J. A. (1980). "Demethyl analogues of psychoactive methoxyphenalkylamines: synthesis and serotonin receptor affinities." *J. Med. Chem*., **23**: 990-994.

Guay, L. A., Musoke, P., Fleming, T., Bagenda, D., Allen M., Nakabiito, J., Bakaki, P., Ducar, C., Deseyve, M., Emel, L., Mirochnick, M., Fowler, M. G., Mofenson, L., Miotti, P., Dransfield, K., Bray, D., Mmiro, F. and Jackson, J. B. (1999). "Intrapartum and neonatal single-dose nevirapine compared with zidovudine for prevention of mother-to-child transmission of HIV-1 in Kampala, Uganda: HIVNET 012 randomised trial." *Lancet*, **354**: 795-802.

Hahn, T. (2002), Hahn Theo, ed., *International Tables for Cryst., Vol. A: Space Group Symmetry*, **A** (5^{th} ed.), Berlin, New York: Springer-Verlag, doi:10.1107/97809553602060000100, ISBN 978-0-7923-6590-7.

Harris, M. (2003). "Efficacy and durability of nevirapine in antiretroviral-experienced Patients." *J. Acquir. Immune Defic. Syndr*., **34**: (Suppl. 1), S53-S58.

Herschhorn, A., Oz-Gleenberg, I. and Hizi, A. (2008). "Mechanism of inhibition of HIV-1 reverse Transcriptase by the novel broad-range DNA-polymerase inhibitor N-{2-[4- (aminosulfonyl)phenyl]ethyl}-2- (2-thienyl)acetamide." *Biochemistry,* **47**: 490-502.

Hogberg, M., Engelhardt, P., Vrang, L. and Zhang, H. (2000). "Bioisosteric modification of PETT-HIV-1 RT-inhibitors: synthesis and biological evaluation." *Bioorg. Med. Chem. Lett.,* **10**: 265-268.

Huang, H., Chopra, R.,Verdine, G. L. and Harrison, S. C. (1998). "Structure of a covalently trapped catalytic complex of HIV-1 Reverse Transcriptase: implications for drug resistance." *Science,* **282**: 1669-1675.

Hunter, R., Younis, Y., Muhanji, C. I., Tanith-Lea, C., Naidoo, J. K., Petersen, M., Chistopher, M. B., Basavapathuni, A. and Anderson, K. S. (2008). "C-2-aryl-O-substituted HI-236 derivatives as a non-nucleoside HIV-1 reverse transcriptase inhibitors." *Bioorg. MediChem.*, **16**: 10270-10280.

Janssen, P. A., Lewi, P. J., Arnold, E., Daeyaert, F., de Jonge, M., Heeres, J., Koymans, L., Vinkers, M., Guillemont, J., Pasquier, E., Kukla, M., Ludovici, D., Andries, K., de Bethune, M. P., Pauwels, R., Das, K., Clark, A. D. Jr., Frenkel, Y. V., Hughes, S. H., Medaer, B., De Knaep, F., Bohets, H., De Clerck, F., Lampo, A., Williams, P. and Stoffels, P. (2005). "In search of a novel anti-HIV drug: multidisciplinary coordination in the discovery of 4-[[4-[[4-[(1E)-2-cyanoethenyl]-2,6-dimethylphenyl]amino]-2-

yrimidinyl]amino]benzonitrile(R278474, rilpivirine).” *J. Med. Chem*., **48**: 1901-1909.

Kennedy, A. R., Kipkorir, Z. R., Muhanji, C. I. and Okoth, M. O., (2010[a]). “4-(Benzyloxy)benzaldehyde.” *Acta Cryst.,* **E66**, o2110.

Kennedy, A. R., Kipkorir, Z. R., Muhanji, C. I. and Okoth, M. O., (2010[b]). “1-Benzyloxy-4-(2-nitroethenyl)benzene.” *Acta Cryst*.. **E66**, o2984–o2985.

Kitchen, C. M., Kitchen, S. G., Dubin, J. A. and Gottlieb, M. S. (2001). “Initial virological and immunologic response to highly active antiretroviral therapy predicts long-term clinical outcome.” *Clin. Infect. Dis*., **33**: 466-472.

Kuno, M., Hannongbua, S. and Morokuma, K. (2003). “Theoretical investigation on nevirapine and HIV-1 reverse transcriptase binding site interaction, based on ONIOM method.” *Chem. Phys. Lett,* **380**: 456-463.

Lange, J. M. (2003). “Efficacy and durability of Nevirapine in antiretroviral drug naive patients.” *J. Acquir.Immune Defic. Syndr.* **34** (suppl. 1):S40-S52.

Li, D., Zhan, P., Clercq, E. and Liu, X. (2012). “Strategies for the design of HIV-1 non-nucleoside reverse transcriptase inhibitors: lessons from the development of seven representative paradigms.” *J. Med. Chem*., **55**: 3595-3613.

Liang, Y. H. and Chen, F. (2007). “ONIOM DFT/PM3 calculations on the interaction between dapivirine and HIV-1 reverse transcriptase, a theoretical study.” *Drug Discov. Ther.*, (**1**): 57-60.

Linda, L. T., Lorenz, K., Mintas, M. and Nagl, A. (1999). “Spirobinaphthopyrans: Synthesis, X-ray Crystal Structures, Separation of Enantiomers, and Barriers to Thermal Racemization.” *Chirality,* **11**: 363 – 372.

Lindberg, J., Sigurdsson, S., Lowgren, S., Andersson, H. O., Sahlberg, C., Noreen, R., Fridborg, K., Zhang, H. and Unge, T. (2002). "Structural basis for the inhibitory efficacy of efavirenz (DMP-266), MSC194 and PNU142721 towards the HIV-1 RT K103N mutant." *Eur. J. Biochem*., **269**: 1670–1677.

Liu, S. X., Tian, X., Zhen, X. L., Li, Z. C. and Han, J. R. (2007). "4-(4-Chlorobenzyloxy)-3-methoxybenzaldehyde." *Acta Cryst.*, **E63**: 4481.

Lodish, H., Baltimore, D., Berk, A., Zipursk, S. L. and Matsudaira, P. (1995). Molecular Cell Biology. 3rd Ed., Scientific American Books, Inc., 330-331.

Ludovici, D. W., Kavash, R. W., Kukla, M. J., Ho, C. Y., Ye, H., De Corte, B. L., Andries, K., de Bethune, M. P., Azijn, H., Pauwels, R., Moereels, H. E., Heeres, J., Koymans, L. M., de Jonge, M. R., Van Aken, K. J., Daeyaert, F. F., Lewi, P. J., Das, K., Arnold, E., Janssen, P. A. (2001). "Evolution of anti-HIV drug candidates. Part 2: Diaryltriazine (DATA) analogues." *Bioorg. Med. Chem. Lett*., **11**, 2229−2234.

Maga G., Radi, M., Gerard, M., Botta, M. and Ennifar E. (2010). "HIV-1 RT Inhibitors with a Novel Mechanism of Action: NNRTIs that Compete with the Nucleotide Substrate." *Viruses*, **2**: 880-899.

Mao, C., Sudbeck, E. A., Venkatachalam, T.K. and Ukun, F. M. (1999). "Rational Design of *N*-[2-(2,5-dimethoxyphenyl)]-*N'*-[2-(5-bromopyridyl)]-thiurea(HI-236 as a potent Non-nucleoside Inhibitor of Drug-Resistant Human Immunodeficiency Virus." *Bioorg. Med. Chem. Lett.*, **9**: 1593.

Mao, C., Rakesh, V., Venkatachalam, T. K., Sudbeck, E. A. and Uckun F. M. (1998). "Structure-Based design of *N*-[2-(1-piperidinylethyl)]-*N*-[2-(5-

bromopyridyl)]-thiourea and *N*-[2-(1-piperazinylethyl)]-*N*-[2-(5-bromopyridyl)]-thiourea as potent Non-Nucleoside inhibitors of HIV-1 Reverse transcriptase." *Bioorg. Med. Chem. lett.*, **8**: 2213-2218.

Marsden, M. D. and Zack, J. A. (2009). "Eradication of HIV: current challenges and new directions." *Antimicrob. Chemother.*, **63**: 7-10.

Mehellou, Y. and De Clercq, E. (2010). "Twenty Six Years of Anti-HIV Drug discovery: Where Do we stand and where do we go?" *J. Med. Chem.*, 53(**2**): 102-106.

Miyasaka, T., Tanaka, H., Baba, M., Hayakawa, H., Walker, R.T., Balzarini, J. and De Clercq, E. (1989). "A novel lead for specific anti-HIV-1 agents: 1-[(2-hydroxyethoxy)methyl]-6-(phenylthio)thymine." *J. Med. Chem.*, **32**: 2507–2509.

Monforte, A., Logoteta, P., Ferro, S., De Luca, L., Iraci, N., Maga, G., De Clercq, E., Pannecouque, C., and Chimirri, A. (2009). "Design, synthesis, and structure–activity relationships of 1,3-dihydrobenzimidazol-2-one analogues as anti-HIV agents." *Bioorg. Med. Chem.*, **17**: 5962-5967.

National Centre in HIV Epidemiology and Clinical Research (2009). "*HIV/AIDS, viral hepatitis and sexually transmissible infections in Australia." Annual surveillance report 2009.* Sydney, Australia, University of New South Wales.

Nunrium, P., Kuno, M., Saen-oon, S. and Hannongbua, S. (2005). "Particular interaction between efavirenz and the HIV-1 reverse transcriptase binding site as explained by the ONIOM2 method." *Chem. Phys. Lett.*, **405**: 198-202.

Pauwels, R., (2004). “New non-nucleoside reverse transcriptase inhibitors (NNRTIs) in development for the treatment of HIV infections.” *Curr. Opin. Pharmacol*., **4**: 437-446.

Pauwels, R., Andries, K., Desmyter, J., Schols, D., Kukla, M. J., Breslin, H. J., Raeymaeckers, A., Van Gelder, J., Woestenborghs, R., Heykants, J. (1990). “Potent and selective inhibition of HIV-1 replication in vitro by a novel series of TIBO derivatives.” *Nature,* **343**, 470−474.

Perelson, A. S. and Ribeiro, R. M. (2008). "Estimating drug efficacy and viral dynamic parameters: HIV and HCV." *Stat. Med*., 27 (**23**): 4647-57.

Prajapati, G. D., Ramajam, R., Yadav, R. M. and Giridhar, R. (2009). “The search for potent, small molecule NNRTIs: A Review.” *Bioorg.Med. Chem.,* **17**: 5744-5762.

Ren, J., Nichols, C., Bird, L., Chamberlin, P., Weaver, K., Sharp, S., Stuart, D. I. and Stammers, D. K. (2001). “Structural Mechanisms of Drug Resistance for mutations at codons 181 and 188 in HIV-1 Reverse transcriptase and the Improved Resistance of Second Generation Non Nucleoside Inhibitors.” *J. Mol. Biol.*, **312**: 795-805.

Ren, J., Nichols, E. C., Chamberlain, K. L., Short, A. S., Chan, H. J., Kleim, P. J. and Stammers, K. D. (**2007**). “Relationship of potency and resilience to drug resistance mutations for GW420867X revealed by crystal structures of inhibitor complexes for wild-type, Leu100Ile, Lys101Glu and Tyr188Cys mutant HIV-1 reverse transcriptase.” *J. Med. Chem*., **50**: 2301-2309.

Roberts, J. D., Bebenek, K., Kunkel, T. A. (1998). "The accuracy of reverse transcriptase from HIV-1." *Science,* **242**: 1171-1173.

Rotich, Z. K. **(**2010) "Towards the synthesis of a thiourea derivative as a potential non-nucleoside reverse transcriptase inhibitor." M.Phil Thesis. Moi University, Eldoret,.

Samuele, A., Kataropoulou, A., Viola, M., Zanoli, S. and Regina, G. L. (2009). "Non-nucleoside HIV-1 transcriptase inhibitors *di-halo*-indolyl aryl sulfones achieve tight binding to drug-resistant mutants by targeting the enzyme-substrate complex." *Antivir. Res.* **81** (1): 47-55.

Sarafianos, S. G., Das, K., Hughes, S. H. and Arnold, E. (2004). "Taking aim at a moving target: designing drugs to inhibit drug-resistant HIV-1 reverse transcriptases." *Curr. Opin. Struct. Biol*., **14**: 716.

Scapin, G., (2006). "Structural biology and drug discovery." *Curr. Pharm. Des.* **12** (17): 2087.

Schiller, D. S. and Youssef-Bessler, M. (2009). "Etravirine: A Second-Generation Nonnucleoside Reverse Transcriptase Inhibitor (NNRTI) Active Against NNRTI-Resistant Strains of HIV." *Clin. Ther.*, **31** (4) : 692-704.

Seminari, E., Castagna, A. and Lazzarin, A. (2008). "Etravirine for the treatment of HIV infection." *Expert Rev. Anti-Infect. Ther*., **6**: 427-433.

UNAIDS, (2011). Report on the global AIDS epidemic. Geneva, UNAIDS.

Venkatachalam T. K., Sudbeck E. and Uckun F. M. (2005). "Structural influence on the solid state intermolecular hydrogen bonding of substituted thioureas." *J. Mol. Struct*., **751**: 41-54.

Venkatachalam, T. K., Mao, C. and Uckun, F. M. (2004). " Effect of stereochemistry On the anti-HIV activity of chiral thiourea compounds." *Bioorg. Med. Chem.*, **12**: 4275-4284.

www.niaid.nih.gov (Accessed on August, 2012).

Yang, Z., Ma, X., Roesky, W. H., Yang, Y., Jimnez-perez, M. V., Magull, J., Arne R. and Jones, G. P. (2007) "Synthesis, characterization, and X-ray single crystal structures of 1,8-Bis(trimethylsilylamino)naphthalene aluminium hydride and methyl devivative." *Eur. J. Inorg. Chem*., 31: 4919 – 4922.

Younis, Y., Hunter, R., Muhanji, C. I., Hale, I., Singh, R., Bailey, C. M., Sullivan, T. J. and Anderson, K. S. (2010). "[d4U]-Spacer-[HI-236] double-drug inhibitors of HIV-1 reverse-transcriptase." *Bioorg. Med. Chem.* **18**: 4661–4673.

APPENDICES

Appendix 1: Crystal data and structure refinement for *N*-[(2(4-benzyloxyphenyl)ethyl]-*tert*-butylcarbamate (**21**)

Identification code	monopnew
Empirical formula	C_{20} H_{25} N O_3
Formula weight	327.41
Temperature	100(2) K
Wavelength	1.54180 Å
Crystal system	Monoclinic Space group P21/c
Unit cell dimensions	a = 11.040(3) Å α= 90°.
	b = 5.0931(12) Å β= 94.493(14)°.
	c = 64.070(16) Å γ = 90°.
	Volume = 3591.4(16) $Å^3$
Z	8
Density (calculated)	1.211 Mg/m^3
Absorption coefficient	0.646 mm^{-1}
F(000)	1408
Crystal size	0.16 x 0.07 x 0.01 mm^3
Theta range for data collection	2.77 to 66.71°.
Index ranges	-13<=h<=12, -5<=k<=5, -76<=l<=76
Reflections collected	15535
Independent reflections	5620 [R(int) = 0.1066]
Completeness to theta = 60.00°,	89.7 %
Absorption correction	Semi-empirical from equivalents
Max. and min. transmission	1.000 and 0.608
Refinement method	Full-matrix least-squares on F^2
Data / restraints / parameters	5620 / 0 / 576
Goodness-of-fit on F^2	1.051

Final R indices [I>2sigma(I)]	R1 = 0.0867, wR2 = 0.2479
R indices (all data)	R1 = 0.1026, wR2 = 0.2699
Largest diff. peak and hole	0.302 and -0.321 e.Å^{-3}

Appendix 2: Atomic coordinates (x 10^4) and equivalent isotropic displacement parameters ($Å^2$x 10^3) for *N*-[(2(4-benzyloxyphenyl)ethyl]-*tert*-butylcarbamate (**21**). U(eq) is defined as one third of the trace of the orthogonalized U^{ij} tensor.

	x	y	z	U(eq)
O(1)	706(2)	5236(5)	1696(1)	44(1)
O(2)	5294(2)	2356(4)	718(1)	33(1)
O(3)	5989(2)	5611(4)	513(1)	34(1)
O(4)	5835(2)	1394(5)	1736(1)	44(1)
O(5)	10294(2)	3011(4)	722(1)	33(1)
O(6)	10925(2)	-416(5)	530(1)	35(1)
N(1)	5003(3)	6669(6)	787(1)	34(1)
N(2)	9884(3)	-1203(6)	807(1)	36(1)
C(1)	1368(3)	5960(8)	1533(1)	38(1)
C(2)	1951(7)	8494(17)	1513(1)	37(2)
C(3)	2582(7)	8946(18)	1336(1)	34(2)
C(4)	2588(3)	7157(7)	1177(1)	36(1)
C(5)	1880(20)	4760(40)	1196(3)	43(4)
C(6)	1349(11)	4360(30)	1360(3)	28(3)
C(7)	3241(3)	7795(7)	985(1)	39(1)
C(8)	4396(3)	6225(7)	978(1)	35(1)
C(9)	5418(3)	4685(6)	676(1)	30(1)
C(10)	6531(3)	3751(7)	371(1)	34(1)
C(11)	7455(3)	2017(7)	490(1)	37(1)
C(12)	7151(4)	5559(7)	224(1)	44(1)
C(13)	5524(3)	2216(7)	248(1)	38(1)
C(14)	907(7)	6434(19)	1890(1)	36(2)
C(15)	-101(12)	5820(30)	2030(2)	40(3)

C(16)	-30(11)	6940(20)	2230(1)	43(3)
C(17)	-999(16)	6460(70)	2352(4)	42(5)
C(18)	-1900(30)	5180(40)	2308(3)	47(5)
C(19)	-2022(12)	3890(30)	2102(2)	46(3)
C(20)	-1130(30)	4120(60)	1967(5)	32(4)
C(21)	6402(3)	634(7)	1562(1)	39(1)
C(22)	6142(3)	1665(7)	1362(1)	39(1)
C(23)	6756(3)	687(7)	1197(1)	39(1)
C(24)	7613(3)	-1285(7)	1223(1)	37(1)
C(25)	7872(3)	-2270(8)	1425(1)	41(1)
C(26)	7271(3)	-1296(8)	1592(1)	44(1)
C(27)	8261(3)	-2261(7)	1038(1)	40(1)
C(28)	9324(3)	-517(7)	998(1)	38(1)
C(29)	10363(3)	665(6)	690(1)	30(1)
C(30)	11484(3)	1296(7)	379(1)	36(1)
C(31)	12441(3)	3040(7)	490(1)	39(1)
C(32)	10499(3)	2817(8)	252(1)	40(1)
C(33)	12082(4)	-632(8)	240(1)	54(1)
C(34)	4945(3)	3436(8)	1710(1)	42(1)
C(35)	4448(3)	3887(7)	1920(1)	40(1)
C(36)	3211(6)	3318(15)	1946(1)	40(2)
C(37)	2776(7)	3640(18)	2143(1)	49(2)
C(38)	3535(4)	4616(9)	2309(1)	54(1)
C(39)	4655(9)	5310(20)	2278(1)	55(2)
C(40)	5140(8)	5023(18)	2081(1)	43(2)
C(36A)	3859(7)	1771(17)	2020(1)	46(2)
C(37A)	3405(8)	2232(18)	2210(1)	52(2)
C(40A)	4658(7)	6180(20)	2024(1)	46(2)
C(39A)	4204(8)	6610(20)	2214(1)	54(2)
C(2A)	2421(8)	7391(18)	1559(1)	39(2)
C(3A)	3014(8)	8047(18)	1384(1)	40(2)
C(6A)	995(13)	4750(40)	1347(3)	39(4)
C(5A)	1686(17)	5450(40)	1165(3)	35(3)

C(14A)	533(7)	7410(16)	1852(1)	40(2)
C(15A)	-237(7)	6322(16)	2009(1)	38(4)
C(16A)	-317(7)	7699(16)	2194(1)	43(3)
C(17A)	-1010(20)	6900(70)	2353(4)	67(8)
C(18A)	-1760(30)	4380(40)	2298(4)	46(5)
C(19A)	-1646(11)	3150(30)	2126(2)	52(3)
C(20A)	-850(30)	4200(70)	1977(5)	50(8)

Appendix 3: Bond lengths [Å] and angles [°] for *N*-[(2(4-benzyloxyphenyl)ethyl]-*tert*-butylcarbamate (**21**).

O(1)-C(1)	1.376(4)
O(1)-C(14)	1.383(8)
O(1)-C(14A)	1.511(8)
O(2)-C(9)	1.225(4)
O(3)-C(9)	1.350(4)
O(3)-C(10)	1.472(4)
O(4)-C(21)	1.377(4)
O(4)-C(34)	1.432(4)
O(5)-C(29)	1.216(4)
O(6)-C(29)	1.355(4)
O(6)-C(30)	1.474(4)
N(1)-C(9)	1.337(4)
N(1)-C(8)	1.457(4)
N(1)-H(1N)	0.81(4)
N(2)-C(29)	1.344(4)
N(2)-C(28)	1.457(4)
N(2)-H(2N)	0.85(5)
C(1)-C(2A)	1.371(8)
C(1)-C(6A)	1.37(2)

C(1)-C(6)	1.375(19)
C(1)-C(2)	1.452(9)
C(2)-C(3)	1.391(10)
C(2)-H(2)	0.9500
C(3)-C(4)	1.367(9)
C(3)-H(3)	0.9500
C(4)-C(5A)	1.32(2)
C(4)-C(3A)	1.441(9)
C(4)-C(5)	1.46(2)
C(4)-C(7)	1.511(4)
C(5)-C(6)	1.26(3)
C(5)-H(5)	0.9500
C(6)-H(6)	0.9500
C(7)-C(8)	1.509(5)
C(7)-H(7A)	0.9900
C(7)-H(7B)	0.9900
C(8)-H(8A)	0.9900
C(8)-H(8B)	0.9900
C(10)-C(11)	1.510(4)
C(10)-C(12)	1.515(5)
C(10)-C(13)	1.525(4)
C(11)-H(11A)	0.9800
C(11)-H(11B)	0.9800
C(11)-H(11C)	0.9800
C(12)-H(12A)	0.9800
C(12)-H(12B)	0.9800
C(12)-H(12C)	0.9800
C(13)-H(13A)	0.9800
C(13)-H(13B)	0.9800
C(13)-H(13C)	0.9800
C(14)-C(15)	1.518(12)
C(14)-H(14A)	0.9900
C(14)-H(14B)	0.9900

C(15)-C(16)	1.398(12)
C(15)-C(20)	1.46(3)
C(16)-C(17)	1.39(2)
C(16)-H(16)	0.9500
C(17)-C(18)	1.20(4)
C(17)-H(17)	0.9500
C(18)-C(19)	1.48(3)
C(18)-H(18)	0.9500
C(19)-C(20)	1.36(4)
C(19)-H(19)	0.9500
C(20)-H(20)	0.9500
C(21)-C(26)	1.377(5)
C(21)-C(22)	1.392(4)
C(22)-C(23)	1.393(4)
C(22)-H(22)	0.9500
C(23)-C(24)	1.381(5)
C(23)-H(23)	0.9500
C(24)-C(25)	1.394(4)
C(24)-C(27)	1.513(4)
C(25)-C(26)	1.398(5)
C(25)-H(25)	0.9500
C(26)-H(26)	0.9500
C(27)-C(28)	1.510(5)
C(27)-H(27A)	0.9900
C(27)-H(27B)	0.9900
C(28)-H(28A)	0.9900
C(28)-H(28B)	0.9900
C(30)-C(33)	1.514(5)
C(30)-C(31)	1.515(5)
C(30)-C(32)	1.517(5)
C(31)-H(31A)	0.9800
C(31)-H(31B)	0.9800
C(31)-H(31C)	0.9800

C(32)-H(32A)	0.9800
C(32)-H(32B)	0.9800
C(32)-H(32C)	0.9800
C(33)-H(33A)	0.9800
C(33)-H(33B)	0.9800
C(33)-H(33C)	0.9800
C(34)-C(35)	1.506(4)
C(34)-H(34A)	0.9900
C(34)-H(34B)	0.9900
C(35)-C(40A)	1.358(9)
C(35)-C(40)	1.363(8)
C(35)-C(36)	1.420(8)
C(35)-C(36A)	1.435(9)
C(36)-C(37)	1.391(9)
C(36)-H(36)	0.9500
C(37)-C(38)	1.392(9)
C(37)-H(37)	0.9500
C(38)-C(39)	1.316(10)
C(38)-C(37A)	1.370(9)
C(38)-C(39A)	1.419(11)
C(38)-H(38)	0.9500
C(39)-C(40)	1.419(11)
C(39)-H(39)	0.9500
C(40)-H(40)	0.9500
C(36A)-C(37A)	1.377(10)
C(36A)-H(36A)	0.9500
C(37A)-H(37A)	0.9500
C(40A)-C(39A)	1.367(11)
C(40A)-H(40A)	0.9500
C(39A)-H(39A)	0.9500
C(2A)-C(3A)	1.386(12)
C(2A)-H(2A)	0.9500
C(3A)-H(3A)	0.9500

C(6A)-C(5A)	1.49(3)
C(6A)-H(6A)	0.9500
C(5A)-H(5A)	0.9500
C(14A)-C(15A)	1.4743
C(14A)-H(14C)	0.9900
C(14A)-H(14D)	0.9900
C(15A)-C(20A)	1.28(4)
C(15A)-C(16A)	1.3895
C(16A)-C(17A)	1.38(3)
C(16A)-H(16A)	0.9500
C(17A)-C(18A)	1.55(4)
C(17A)-H(17A)	0.9500
C(18A)-C(19A)	1.28(3)
C(18A)-H(18A)	0.9500
C(19A)-C(20A)	1.45(4)
C(19A)-H(19A)	0.9500
C(20A)-H(20A)	0.9500
C(1)-O(1)-C(14)	120.5(4)
C(1)-O(1)-C(14A)	114.1(4)
C(14)-O(1)-C(14A)	26.6(3)
C(9)-O(3)-C(10)	119.5(2)
C(21)-O(4)-C(34)	117.6(2)
C(29)-O(6)-C(30)	119.7(2)
C(9)-N(1)-C(8)	121.9(3)
C(9)-N(1)-H(1N)	122(2)
C(8)-N(1)-H(1N)	116(2)
C(29)-N(2)-C(28)	120.6(3)
C(29)-N(2)-H(2N)	118(3)
C(28)-N(2)-H(2N)	119(3)
C(2A)-C(1)-C(6A)	122.7(9)
C(2A)-C(1)-C(6)	112.0(7)
C(6A)-C(1)-C(6)	18.4(8)
C(2A)-C(1)-O(1)	123.0(4)

C(6A)-C(1)-O(1)	113.4(9)
C(6)-C(1)-O(1)	118.7(7)
C(2A)-C(1)-C(2)	33.0(4)
C(6A)-C(1)-C(2)	115.4(10)
C(6)-C(1)-C(2)	115.8(8)
O(1)-C(1)-C(2)	124.9(4)
C(3)-C(2)-C(1)	118.2(6)
C(3)-C(2)-H(2)	120.9
C(1)-C(2)-H(2)	120.9
C(4)-C(3)-C(2)	121.8(7)
C(4)-C(3)-H(3)	119.1
C(2)-C(3)-H(3)	119.1
C(5A)-C(4)-C(3)	115.8(10)
C(5A)-C(4)-C(3A)	116.9(9)
C(3)-C(4)-C(3A)	29.2(4)
C(5A)-C(4)-C(5)	17.6(9)
C(3)-C(4)-C(5)	117.6(10)
C(3A)-C(4)-C(5)	109.1(9)
C(5A)-C(4)-C(7)	119.9(9)
C(3)-C(4)-C(7)	119.7(5)
C(3A)-C(4)-C(7)	122.6(5)
C(5)-C(4)-C(7)	122.5(10)
C(6)-C(5)-C(4)	119.4(19)
C(6)-C(5)-H(5)	120.3
C(4)-C(5)-H(5)	120.3
C(5)-C(6)-C(1)	126.6(16)
C(5)-C(6)-H(6)	116.7
C(1)-C(6)-H(6)	116.7
C(8)-C(7)-C(4)	111.6(3)
C(8)-C(7)-H(7A)	109.3
C(4)-C(7)-H(7A)	109.3
C(8)-C(7)-H(7B)	109.3
C(4)-C(7)-H(7B)	109.3

H(7A)-C(7)-H(7B)	108.0
N(1)-C(8)-C(7)	112.8(3)
N(1)-C(8)-H(8A)	109.0
C(7)-C(8)-H(8A)	109.0
N(1)-C(8)-H(8B)	109.0
C(7)-C(8)-H(8B)	109.0
H(8A)-C(8)-H(8B)	107.8
O(2)-C(9)-N(1)	124.7(3)
O(2)-C(9)-O(3)	124.9(3)
N(1)-C(9)-O(3)	110.4(3)
O(3)-C(10)-C(11)	110.8(2)
O(3)-C(10)-C(12)	102.5(3)
C(11)-C(10)-C(12)	110.3(3)
O(3)-C(10)-C(13)	109.4(2)
C(11)-C(10)-C(13)	113.3(3)
C(12)-C(10)-C(13)	109.9(2)
C(10)-C(11)-H(11A)	109.5
C(10)-C(11)-H(11B)	109.5
H(11A)-C(11)-H(11B)	109.5
C(10)-C(11)-H(11C)	109.5
H(11A)-C(11)-H(11C)	109.5
H(11B)-C(11)-H(11C)	109.5
C(10)-C(12)-H(12A)	109.5
C(10)-C(12)-H(12B)	109.5
H(12A)-C(12)-H(12B)	109.5
C(10)-C(12)-H(12C)	109.5
H(12A)-C(12)-H(12C)	109.5
H(12B)-C(12)-H(12C)	109.5
C(10)-C(13)-H(13A)	109.5
C(10)-C(13)-H(13B)	109.5
H(13A)-C(13)-H(13B)	109.5
C(10)-C(13)-H(13C)	109.5
H(13A)-C(13)-H(13C)	109.5

H(13B)-C(13)-H(13C)	109.5
O(1)-C(14)-C(15)	111.5(7)
O(1)-C(14)-H(14A)	109.3
C(15)-C(14)-H(14A)	109.3
O(1)-C(14)-H(14B)	109.3
C(15)-C(14)-H(14B)	109.3
H(14A)-C(14)-H(14B)	108.0
C(16)-C(15)-C(20)	118.8(15)
C(16)-C(15)-C(14)	117.8(9)
C(20)-C(15)-C(14)	123.4(15)
C(17)-C(16)-C(15)	116.7(14)
C(17)-C(16)-H(16)	121.6
C(15)-C(16)-H(16)	121.6
C(18)-C(17)-C(16)	129(2)
C(18)-C(17)-H(17)	115.7
C(16)-C(17)-H(17)	115.7
C(17)-C(18)-C(19)	118(2)
C(17)-C(18)-H(18)	121.1
C(19)-C(18)-H(18)	121.1
C(20)-C(19)-C(18)	121(2)
C(20)-C(19)-H(19)	119.7
C(18)-C(19)-H(19)	119.7
C(19)-C(20)-C(15)	118(2)
C(19)-C(20)-H(20)	121.2
C(15)-C(20)-H(20)	121.2
O(4)-C(21)-C(26)	116.1(3)
O(4)-C(21)-C(22)	124.4(3)
C(26)-C(21)-C(22)	119.5(3)
C(21)-C(22)-C(23)	119.1(3)
C(21)-C(22)-H(22)	120.5
C(23)-C(22)-H(22)	120.5
C(24)-C(23)-C(22)	122.5(3)
C(24)-C(23)-H(23)	118.8

C(22)-C(23)-H(23)	118.8
C(23)-C(24)-C(25)	117.6(3)
C(23)-C(24)-C(27)	120.3(3)
C(25)-C(24)-C(27)	122.1(3)
C(24)-C(25)-C(26)	120.7(3)
C(24)-C(25)-H(25)	119.7
C(26)-C(25)-H(25)	119.7
C(21)-C(26)-C(25)	120.6(3)
C(21)-C(26)-H(26)	119.7
C(25)-C(26)-H(26)	119.7
C(28)-C(27)-C(24)	111.3(3)
C(28)-C(27)-H(27A)	109.4
C(24)-C(27)-H(27A)	109.4
C(28)-C(27)-H(27B)	109.4
C(24)-C(27)-H(27B)	109.4
H(27A)-C(27)-H(27B)	108.0
N(2)-C(28)-C(27)	113.0(3)
N(2)-C(28)-H(28A)	109.0
C(27)-C(28)-H(28A)	109.0
N(2)-C(28)-H(28B)	109.0
C(27)-C(28)-H(28B)	109.0
H(28A)-C(28)-H(28B)	107.8
O(5)-C(29)-N(2)	124.6(3)
O(5)-C(29)-O(6)	124.6(3)
N(2)-C(29)-O(6)	110.8(3)
O(6)-C(30)-C(33)	103.2(3)
O(6)-C(30)-C(31)	110.5(2)
C(33)-C(30)-C(31)	109.7(3)
O(6)-C(30)-C(32)	109.6(3)
C(33)-C(30)-C(32)	110.1(3)
C(31)-C(30)-C(32)	113.3(3)
C(30)-C(31)-H(31A)	109.5
C(30)-C(31)-H(31B)	109.5

H(31A)-C(31)-H(31B)	109.5
C(30)-C(31)-H(31C)	109.5
H(31A)-C(31)-H(31C)	109.5
H(31B)-C(31)-H(31C)	109.5
C(30)-C(32)-H(32A)	109.5
C(30)-C(32)-H(32B)	109.5
H(32A)-C(32)-H(32B)	109.5
C(30)-C(32)-H(32C)	109.5
H(32A)-C(32)-H(32C)	109.5
H(32B)-C(32)-H(32C)	109.5
C(30)-C(33)-H(33A)	109.5
C(30)-C(33)-H(33B)	109.5
H(33A)-C(33)-H(33B)	109.5
C(30)-C(33)-H(33C)	109.5
H(33A)-C(33)-H(33C)	109.5
H(33B)-C(33)-H(33C)	109.5
O(4)-C(34)-C(35)	107.7(3)
O(4)-C(34)-H(34A)	110.2
C(35)-C(34)-H(34A)	110.2
O(4)-C(34)-H(34B)	110.2
C(35)-C(34)-H(34B)	110.2
H(34A)-C(34)-H(34B)	108.5
C(40A)-C(35)-C(40)	36.7(4)
C(40A)-C(35)-C(36)	104.2(5)
C(40)-C(35)-C(36)	118.9(5)
C(40A)-C(35)-C(36A)	119.5(5)
C(40)-C(35)-C(36A)	103.2(5)
C(36)-C(35)-C(36A)	47.1(4)
C(40A)-C(35)-C(34)	120.7(5)
C(40)-C(35)-C(34)	121.1(4)
C(36)-C(35)-C(34)	119.8(4)
C(36A)-C(35)-C(34)	119.5(4)
C(37)-C(36)-C(35)	119.2(6)

C(37)-C(36)-H(36)	120.4
C(35)-C(36)-H(36)	120.4
C(36)-C(37)-C(38)	120.2(7)
C(36)-C(37)-H(37)	119.9
C(38)-C(37)-H(37)	119.9
C(39)-C(38)-C(37A)	103.6(6)
C(39)-C(38)-C(37)	119.9(5)
C(37A)-C(38)-C(37)	45.4(5)
C(39)-C(38)-C(39A)	38.5(5)
C(37A)-C(38)-C(39A)	118.5(5)
C(37)-C(38)-C(39A)	103.4(5)
C(39)-C(38)-H(38)	120.1
C(37A)-C(38)-H(38)	117.8
C(37)-C(38)-H(38)	120.1
C(39A)-C(38)-H(38)	123.4
C(38)-C(39)-C(40)	122.0(7)
C(38)-C(39)-H(39)	119.0
C(40)-C(39)-H(39)	119.0
C(35)-C(40)-C(39)	119.3(7)
C(35)-C(40)-H(40)	120.4
C(39)-C(40)-H(40)	120.4
C(37A)-C(36A)-C(35)	118.5(7)
C(37A)-C(36A)-H(36A)	120.8
C(35)-C(36A)-H(36A)	120.8
C(38)-C(37A)-C(36A)	121.8(7)
C(38)-C(37A)-H(37A)	119.1
C(36A)-C(37A)-H(37A)	119.1
C(35)-C(40A)-C(39A)	120.9(8)
C(35)-C(40A)-H(40A)	119.5
C(39A)-C(40A)-H(40A)	119.5
C(40A)-C(39A)-C(38)	120.4(8)
C(40A)-C(39A)-H(39A)	119.8
C(38)-C(39A)-H(39A)	119.8

C(1)-C(2A)-C(3A)	118.5(6)
C(1)-C(2A)-H(2A)	120.7
C(3A)-C(2A)-H(2A)	120.7
C(2A)-C(3A)-C(4)	121.8(8)
C(2A)-C(3A)-H(3A)	119.1
C(4)-C(3A)-H(3A)	119.1
C(1)-C(6A)-C(5A)	115.7(16)
C(1)-C(6A)-H(6A)	122.1
C(5A)-C(6A)-H(6A)	122.1
C(4)-C(5A)-C(6A)	122.8(17)
C(4)-C(5A)-H(5A)	118.6
C(6A)-C(5A)-H(5A)	118.6
C(15A)-C(14A)-O(1)	106.4(3)
C(15A)-C(14A)-H(14C)	110.4
O(1)-C(14A)-H(14C)	110.4
C(15A)-C(14A)-H(14D)	110.4
O(1)-C(14A)-H(14D)	110.4
H(14C)-C(14A)-H(14D)	108.6
C(20A)-C(15A)-C(16A)	119.3(17)
C(20A)-C(15A)-C(14A)	122.5(17)
C(16A)-C(15A)-C(14A)	118.2
C(17A)-C(16A)-C(15A)	123.8(15)
C(17A)-C(16A)-H(16A)	118.1
C(15A)-C(16A)-H(16A)	118.1
C(16A)-C(17A)-C(18A)	113(2)
C(16A)-C(17A)-H(17A)	123.5
C(18A)-C(17A)-H(17A)	123.5
C(19A)-C(18A)-C(17A)	121(2)
C(19A)-C(18A)-H(18A)	119.6
C(17A)-C(18A)-H(18A)	119.6
C(18A)-C(19A)-C(20A)	119(2)
C(18A)-C(19A)-H(19A)	120.3
C(20A)-C(19A)-H(19A)	120.3

C(15A)-C(20A)-C(19A)	123(3)
C(15A)-C(20A)-H(20A)	118.3
C(19A)-C(20A)-H(20A)	118.3

Symmetry transformations used to generate equivalent atoms:

Appendix 4: Anisotropic displacement parameters ($Å^2 x\ 10^3$) for *N*-[(2(4-benzyloxyphenyl)ethyl]-*tert*-butylcarbamate (**21**). The anisotropic displacement factor exponent takes the form: $-2\pi^2[h^2 a^{*2} U^{11} + ... + 2 h k a^* b^* U^{12}]$

	U^{11}	U^{22}	U^{33}	U^{23}	U^{13}	U^{12}
O(1)	43(1)	56(2)	34(1)	-4(1)	10(1)	-7(1)
O(2)	35(1)	26(1)	38(1)	1(1)	4(1)	0(1)
O(3)	40(1)	26(1)	37(1)	1(1)	10(1)	4(1)
O(4)	44(1)	56(2)	34(1)	1(1)	7(1)	9(1)
O(5)	36(1)	28(1)	37(1)	-3(1)	4(1)	1(1)
O(6)	41(1)	29(1)	38(1)	0(1)	14(1)	-2(1)
N(1)	40(2)	23(2)	39(1)	3(1)	10(1)	0(1)
N(2)	43(2)	28(2)	39(1)	-2(1)	12(1)	-3(1)
C(1)	37(2)	44(2)	34(2)	0(1)	6(1)	-3(2)
C(2)	43(4)	31(5)	39(4)	-2(3)	12(3)	6(4)
C(3)	34(4)	27(5)	44(4)	-5(3)	13(3)	-3(4)
C(4)	37(2)	36(2)	36(2)	2(1)	6(1)	6(2)
C(5)	67(9)	31(8)	30(7)	0(5)	-8(5)	7(6)
C(6)	21(8)	23(5)	39(5)	-2(3)	6(5)	-8(5)
C(7)	42(2)	33(2)	43(2)	6(1)	9(1)	8(2)
C(8)	37(2)	34(2)	33(1)	4(1)	8(1)	3(2)
C(9)	28(2)	28(2)	32(1)	1(1)	0(1)	3(1)

C(10)	35(2)	31(2)	37(2)	-1(1)	8(1)	5(1)
C(11)	30(2)	35(2)	46(2)	-4(1)	4(1)	2(2)
C(12)	51(2)	35(2)	48(2)	-2(1)	20(1)	4(2)
C(13)	35(2)	41(2)	37(2)	-3(1)	3(1)	5(2)
C(14)	33(4)	39(6)	37(4)	-5(3)	7(3)	3(4)
C(15)	39(6)	43(6)	38(5)	10(4)	0(4)	6(5)
C(16)	50(6)	48(6)	31(4)	-1(4)	3(4)	8(5)
C(17)	29(8) 13(8)	60(12)	41(8)	3(6)	19(6)	
C(18)	68(10) 10(9)	39(14)	38(5)	-1(7)	25(4)	
C(19)	30(6) 11(4)	42(7)	66(7)	7(4)	6(5)	
C(20)	21(11)	38(7)	37(5)	-3(4)	-2(6)	-13(6)
C(21)	41(2)	43(2)	32(1)	-4(1)	6(1)	-5(2)
C(22)	39(2)	41(2)	37(2)	0(1)	2(1)	2(2)
C(23)	41(2)	45(2)	30(1)	0(1)	4(1)	-2(2)
C(24)	36(2)	37(2)	37(2)	-3(1)	7(1)	-9(2)
C(25)	37(2)	44(2)	43(2)	4(1)	10(1)	3(2)
C(26)	44(2)	54(2)	36(2)	7(1)	5(1)	6(2)
C(27)	46(2)	35(2)	39(2)	-4(1)	7(1)	-4(2)
C(28)	43(2)	33(2)	38(2)	-5(1)	11(1)	-7(2)
C(29)	29(2)	29(2)	32(1)	-2(1)	1(1)	-1(1)
C(30)	37(2)	36(2)	37(2)	3(1)	13(1)	-1(2)
C(31)	28(2)	43(2)	47(2)	9(1)	4(1)	1(2)

C(32)	37(2)	49(2)	35(2)	6(1)	2(1)	-7(2)
C(33)	77(3)	32(2)	59(2)	2(2)	37(2)	-2(2)
C(34)	42(2)	47(2)	36(2)	-3(1)	3(1)	3(2)
C(35)	40(2)	45(2)	36(2)	-1(1)	3(1)	5(2)
C(36)	35(4)	39(4)	44(3)	-7(3)	2(3)	6(3)
C(37)	41(4) 10(4)	50(5)	58(4)	4(3)	15(3)	
C(38)	59(3) 21(2)	64(3)	40(2)	5(2)	11(2)	
C(39)	71(6)	61(6)	33(4)	-4(4)	-1(3)	-7(5)
C(40)	37(4)	46(5)	46(4)	-11(3)	4(3)	1(4)
C(36A)	45(4)	47(5)	46(3)	-3(3)	5(3)	1(4)
C(37A)	62(5)	47(5)	50(4)	1(3)	21(3)	-4(5)
C(40A)	31(4)	53(6)	53(4)	-5(4)	-1(3)	7(4)
C(39A)	65(5) 19(5)	58(6)	39(4)	-5(4)	-1(3)	
C(2A)	43(4)	38(5)	36(3)	-5(3)	3(3)	-3(4)
C(3A)	38(5) 10(4)	31(5)	51(5)	-5(3)	7(3)	
C(6A)	16(7)	60(8)	40(5)	-10(4)	2(5)	5(5)
C(5A)	40(6)	46(10)	18(4)	8(5)	-2(4)	0(6)
C(14A)	49(5) 16(4)	38(6)	35(4)	-2(3)	7(3)	
C(15A)	42(7) 12(5)	49(8)	24(5)	6(4)	4(4)	
C(16A)	48(6)	44(7)	37(4)	6(4)	3(4)	3(5)
C(17A)	108(18)	60(12)	32(8)	-5(6)	6(8)	-16(10)

C(18A) 48(8) 4(7)	28(12)	65(8)	2(7)	24(5)	-
C(19A) 36(7) 5(6)	73(11)	47(5)	10(6)	8(5)	-
C(20A) 30(15) 17(8)	81(12)	40(7)	7(6)	3(7)	-

Appendix 5: Hydrogen coordinates (x 10^4) and isotropic displacement parameters ($Å^2$x 10^3)

for *N*-[(2(4-benzyloxyphenyl)ethyl]-*tert*-butylcarbamate (**21**).

	x	y	z	U(eq)
H(2)	1904	9807	1617	44
H(3)	3019	10541	1326	41
H(5)	1821	3517	1085	52
H(6)	889	2787	1364	33
H(7A)	2698	7413	858	47
H(7B)	3437	9691	985	47
H(8A)	4957	6699	1100	41
H(8B)	4203	4334	989	41
H(11A)	7983	3094	585	55
H(11B)	7947	1119	391	55
H(11C)	7035	712	570	55
H(12A)	6558	6814	161	66
H(12B)	7489	4519	114	66
H(12C)	7807	6514	303	66
H(13A)	5157	981	342	56
H(13B)	5865	1243	135	56
H(13C)	4901	3437	190	56
H(14A)	958	8358	1870	43
H(14B)	1693	5826	1958	43
H(16)	646	7976	2280	52
H(17)	-942	7248	2486	51
H(18)	-2511	5010	2404	57

H(19)	-2728	2881	2062	55
H(20)	-1179	3211	1837	38
H(22)	5554	3018	1339	47
H(23)	6578	1402	1061	47
H(25)	8462	-3616	1448	49
H(26)	7464	-1973	1729	53
H(27A)	8555	-4073	1067	48
H(27B)	7684	-2305	912	48
H(28A)	9043	1328	988	45
H(28B)	9942	-643	1118	45
H(31A)	12045	4477	560	59
H(31B)	12965	3765	388	59
H(31C)	12933	2004	594	59
H(32A)	9857	1608	199	60
H(32B)	10849	3684	134	60
H(32C)	10156	4143	341	60
H(33A)	12719	-1598	322	81
H(33B)	12442	323	127	81
H(33C)	11472	-1871	179	81
H(34A)	4283	2911	1605	50
H(34B)	5320	5067	1661	50
H(36)	2686	2725	1831	47
H(37)	1959	3192	2164	59
H(38)	3243	4783	2443	65
H(39)	5155	6020	2391	66
H(40)	5939	5618	2061	51
H(36A)	3784	90	1956	55
H(37A)	2991	860	2276	63
H(40A)	5126	7514	1965	55
H(39A)	4338	8246	2283	65
H(2A)	2737	7920	1695	47
H(3A)	3721	9113	1400	48
H(6A)	338	3541	1336	46

H(5A)	1468	4629	1034	42
H(14C)	1327	7976	1920	48
H(14D)	133	8942	1781	48
H(16A)	133	9284	2213	52
H(17A)	-1030	7794	2483	80
H(18A)	-2311	3736	2393	55
H(19A)	-2077	1563	2097	62
H(20A)	-787	3281	1850	60
H(1N)	5110(30)	8200(80)	756(5)	26(9)
H(2N)	10070(40)	-2790(90)	785(6)	51(12)

Appendix 6: Torsion angles [°] for *N*-[(2(4-benzyloxyphenyl)ethyl]-*tert*-butylcarbamate (**21**).

C(14)-O(1)-C(1)-C(2A)	15.6(8)
C(14A)-O(1)-C(1)-C(2A)	44.8(7)
C(14)-O(1)-C(1)-C(6A)	-175.0(8)
C(14A)-O(1)-C(1)-C(6A)	-145.8(7)
C(14)-O(1)-C(1)-C(6)	165.3(8)
C(14A)-O(1)-C(1)-C(6)	-165.5(7)
C(14)-O(1)-C(1)-C(2)	-24.4(7)
C(14A)-O(1)-C(1)-C(2)	4.8(6)
C(2A)-C(1)-C(2)-C(3)	82.3(10)
C(6A)-C(1)-C(2)-C(3)	-29.3(11)
C(6)-C(1)-C(2)-C(3)	-8.8(11)
O(1)-C(1)-C(2)-C(3)	-179.4(6)
C(1)-C(2)-C(3)-C(4)	4.8(12)
C(2)-C(3)-C(4)-C(5A)	21.2(11)
C(2)-C(3)-C(4)-C(3A)	-78.2(13)
C(2)-C(3)-C(4)-C(5)	1.6(12)
C(2)-C(3)-C(4)-C(7)	177.3(6)
C(5A)-C(4)-C(5)-C(6)	-92(6)
C(3)-C(4)-C(5)-C(6)	-3.8(16)
C(3A)-C(4)-C(5)-C(6)	26.8(16)
C(7)-C(4)-C(5)-C(6)	-179.4(10)
C(4)-C(5)-C(6)-C(1)	-1(2)
C(2A)-C(1)-C(6)-C(5)	-28.7(16)
C(6A)-C(1)-C(6)-C(5)	100(5)
O(1)-C(1)-C(6)-C(5)	178.4(12)
C(2)-C(1)-C(6)-C(5)	7.2(16)
C(5A)-C(4)-C(7)-C(8)	-97.2(8)
C(3)-C(4)-C(7)-C(8)	107.8(5)
C(3A)-C(4)-C(7)-C(8)	73.6(6)

C(5)-C(4)-C(7)-C(8)	-76.8(8)
C(9)-N(1)-C(8)-C(7)	-133.3(3)
C(4)-C(7)-C(8)-N(1)	176.1(3)
C(8)-N(1)-C(9)-O(2)	2.9(5)
C(8)-N(1)-C(9)-O(3)	-177.2(2)
C(10)-O(3)-C(9)-O(2)	-0.8(4)
C(10)-O(3)-C(9)-N(1)	179.3(2)
C(9)-O(3)-C(10)-C(11)	-57.9(3)
C(9)-O(3)-C(10)-C(12)	-175.6(3)
C(9)-O(3)-C(10)-C(13)	67.8(3)
C(1)-O(1)-C(14)-C(15)	166.7(8)
C(14A)-O(1)-C(14)-C(15)	83.4(14)
O(1)-C(14)-C(15)-C(16)	-178.9(10)
O(1)-C(14)-C(15)-C(20)	1(2)
C(20)-C(15)-C(16)-C(17)	-4(3)
C(14)-C(15)-C(16)-C(17)	176.6(16)
C(15)-C(16)-C(17)-C(18)	1(4)
C(16)-C(17)-C(18)-C(19)	1(4)
C(17)-C(18)-C(19)-C(20)	1(3)
C(18)-C(19)-C(20)-C(15)	-4(3)
C(16)-C(15)-C(20)-C(19)	5(3)
C(14)-C(15)-C(20)-C(19)	-175.0(17)
C(34)-O(4)-C(21)-C(26)	178.7(3)
C(34)-O(4)-C(21)-C(22)	-1.9(5)
O(4)-C(21)-C(22)-C(23)	-178.3(3)
C(26)-C(21)-C(22)-C(23)	1.0(5)
C(21)-C(22)-C(23)-C(24)	0.3(5)
C(22)-C(23)-C(24)-C(25)	-1.0(5)
C(22)-C(23)-C(24)-C(27)	-179.5(3)
C(23)-C(24)-C(25)-C(26)	0.5(5)
C(27)-C(24)-C(25)-C(26)	179.0(3)
O(4)-C(21)-C(26)-C(25)	177.9(3)
C(22)-C(21)-C(26)-C(25)	-1.5(6)

C(24)-C(25)-C(26)-C(21)	0.7(6)
C(23)-C(24)-C(27)-C(28)	83.0(4)
C(25)-C(24)-C(27)-C(28)	-95.4(4)
C(29)-N(2)-C(28)-C(27)	146.2(3)
C(24)-C(27)-C(28)-N(2)	-173.1(3)
C(28)-N(2)-C(29)-O(5)	-5.7(5)
C(28)-N(2)-C(29)-O(6)	174.7(3)
C(30)-O(6)-C(29)-O(5)	-1.3(4)
C(30)-O(6)-C(29)-N(2)	178.2(2)
C(29)-O(6)-C(30)-C(33)	175.9(3)
C(29)-O(6)-C(30)-C(31)	58.7(4)
C(29)-O(6)-C(30)-C(32)	-66.9(3)
C(21)-O(4)-C(34)-C(35)	179.2(3)
O(4)-C(34)-C(35)-C(40A)	113.4(5)
O(4)-C(34)-C(35)-C(40)	70.4(6)
O(4)-C(34)-C(35)-C(36)	-114.7(5)
O(4)-C(34)-C(35)-C(36A)	-60.0(5)
C(40A)-C(35)-C(36)-C(37)	-44.0(8)
C(40)-C(35)-C(36)-C(37)	-7.6(10)
C(36A)-C(35)-C(36)-C(37)	73.3(8)
C(34)-C(35)-C(36)-C(37)	177.4(6)
C(35)-C(36)-C(37)-C(38)	2.8(11)
C(36)-C(37)-C(38)-C(39)	2.0(12)
C(36)-C(37)-C(38)-C(37A)	-77.3(9)
C(36)-C(37)-C(38)-C(39A)	39.7(9)
C(37A)-C(38)-C(39)-C(40)	44.2(11)
C(37)-C(38)-C(39)-C(40)	-1.9(14)
C(39A)-C(38)-C(39)-C(40)	-74.8(10)
C(40A)-C(35)-C(40)-C(39)	81.9(12)
C(36)-C(35)-C(40)-C(39)	7.8(11)
C(36A)-C(35)-C(40)-C(39)	-40.2(10)
C(34)-C(35)-C(40)-C(39)	-177.3(7)
C(38)-C(39)-C(40)-C(35)	-3.1(15)

C(40A)-C(35)-C(36A)-C(37A)	6.9(10)
C(40)-C(35)-C(36A)-C(37A)	42.5(9)
C(36)-C(35)-C(36A)-C(37A)	-74.9(8)
C(34)-C(35)-C(36A)-C(37A)	-179.6(6)
C(39)-C(38)-C(37A)-C(36A)	-41.2(10)
C(37)-C(38)-C(37A)-C(36A)	77.6(9)
C(39A)-C(38)-C(37A)-C(36A)	-2.9(12)
C(35)-C(36A)-C(37A)-C(38)	-2.0(12)
C(40)-C(35)-C(40A)-C(39A)	-78.2(11)
C(36)-C(35)-C(40A)-C(39A)	41.5(9)
C(36A)-C(35)-C(40A)-C(39A)	-6.9(11)
C(34)-C(35)-C(40A)-C(39A)	179.7(7)
C(35)-C(40A)-C(39A)-C(38)	1.9(12)
C(39)-C(38)-C(39A)-C(40A)	78.4(11)
C(37A)-C(38)-C(39A)-C(40A)	3.1(11)
C(37)-C(38)-C(39A)-C(40A)	-43.2(10)
C(6A)-C(1)-C(2A)-C(3A)	12.2(13)
C(6)-C(1)-C(2A)-C(3A)	29.2(11)
O(1)-C(1)-C(2A)-C(3A)	-179.3(6)
C(2)-C(1)-C(2A)-C(3A)	-74.7(10)
C(1)-C(2A)-C(3A)-C(4)	-3.2(12)
C(5A)-C(4)-C(3A)-C(2A)	-7.3(12)
C(3)-C(4)-C(3A)-C(2A)	88.0(14)
C(5)-C(4)-C(3A)-C(2A)	-24.6(12)
C(7)-C(4)-C(3A)-C(2A)	-178.4(7)
C(2A)-C(1)-C(6A)-C(5A)	-10.1(15)
C(6)-C(1)-C(6A)-C(5A)	-69(4)
O(1)-C(1)-C(6A)-C(5A)	-179.6(9)
C(2)-C(1)-C(6A)-C(5A)	26.9(13)
C(3)-C(4)-C(5A)-C(6A)	-23.3(15)
C(3A)-C(4)-C(5A)-C(6A)	9.3(16)
C(5)-C(4)-C(5A)-C(6A)	77(5)
C(7)-C(4)-C(5A)-C(6A)	-179.3(10)

C(1)-C(6A)-C(5A)-C(4)	-1.2(18)
C(1)-O(1)-C(14A)-C(15A)	177.35(19)
C(14)-O(1)-C(14A)-C(15A)	-72.3(12)
O(1)-C(14A)-C(15A)-C(20A)	-15.9(18)
O(1)-C(14A)-C(15A)-C(16A)	165.9(3)
C(20A)-C(15A)-C(16A)-C(17A)	1(2)
C(14A)-C(15A)-C(16A)-C(17A)	179.7(14)
C(15A)-C(16A)-C(17A)-C(18A)	-3(3)
C(16A)-C(17A)-C(18A)-C(19A)	4(3)
C(17A)-C(18A)-C(19A)-C(20A)	-3(3)
C(16A)-C(15A)-C(20A)-C(19A)	0(3)
C(14A)-C(15A)-C(20A)-C(19A)	-177.9(17)
C(18A)-C(19A)-C(20A)-C(15A)	1(4)

Symmetry transformations used to generate equivalent atoms: